Excitation functions of some nuclear processes induced by deuteron, ^{3}He- and alpha particles on ^{nat}Ne and Ar:

Production of ^{22,24}Na and ^{43}K and their application for tracing the sap flow of oak trees

PhD thesis

by

András Fenyvesi, dr. univ.

Lajos Kossuth University
Debrecen, Hungary

1997

Ezen értekezést a KLTE **"Fizika"** doktori program **"Magfizika"** alprogramja keretében készítettem **1995-1997** között és ezúton benyújtom a KLTE doktori PhD fokozatának elnyerése céljából.

Debrecen, 1997. augusztus 8.

dr. univ. Fenyvesi András
doktorjelölt

Tanúsítom, hogy **dr. univ. Fenyvesi András** doktorjelölt **1995-1997** között a fent megnevezett doktori alprogram keretében irányításommal végezte munkáját. Az értekezésben foglaltak a jelölt önálló munkáján alapulnak, az eredményekhez önálló alkotó tevékenységével meghatározóan hozzájárult. Az értekezés elfogadását javaslom.

Debrecen, 1997. augusztus 8.

Dr. Tárkányi Ferenc
témavezető

The following publications are related to the contents of this thesis:

Papers dealing with measurements of excitation functions of some relevant nuclear processes:

1 **Fenyvesi, A.**, Tárkányi, F., Szelecsényi, F., Takács, S., Szűcs, Z., Molnár, T., Sudár, S.
Measurement of excitation function and thick target yield of the ^{40}Ar(α,p)^{43}K reaction
Proceedings of the International Conference on Nuclear Data for Science and Technology, Gatlinburg, Tennessee, May 9-13, 1994, Ed.: J. K. Dickens, American Nuclear Society, Inc., 555 N. Kensington Ave., La Grange Park, Illinois 60525, USA, 1994, pp. 406-408.

2 **Fenyvesi, A.**, Tárkányi, F., Szelecsényi, F., Takács, S., Szűcs, Z., Molnár, T., Sudár, S.
Excitation function and thick target yield of the ^{40}Ar(α,p)^{43}K reaction: production of ^{43}K
Applied Radiation and Isotopes **46**, 1413 (1995).

3 **Fenyvesi, A.**, Merchel, S., Takács, S., Szelecsényi, F., Tárkányi, F. and Qaim, S. M.
Excitation Functions of ^{nat}Ne(^{3}He,x)^{22,24}Na and ^{nat}Ne(α,x)^{22,24}Na Processes: Investigation of Production of ^{22}Na and ^{24}Na at a Medium-Sized Cyclotron
Radiochimica Acta (accepted for publication).

4 **Fenyvesi, A.**, Takács, S., Merchel, S., Pető, G., Szelecsényi, F., Molnár, T., Tárkányi, F. and Qaim, S. M.
Excitation Functions of Charged Particle Induced Reactions on Neon: Relevance to the Production of ^{22,24}Na and ^{18}F
Presented at the *International Conference on Nuclear Data for Science and Technology, 19-24 May, 1997, Trieste, Italy* and submitted for publication in the Proceedings of the Conference (in press).

Papers dealing with the applications of ^{24}Na and ^{43}K radioisotopes and computer tomography for studying the water status of healthy and unhealthy mature oak trees:

5 Béres, Cs., **Fenyvesi, A.**, Jakucs, P., Mahunka, I., Kovács, Z., Molnár, T., Szabó, L., Ditrói, F.
Application of an MGC-20 cyclotron and methods of radioecology in solution of problems of forestry and the wood industry
Nuclear Instruments and Methods in Physics Research **B 43**, 101(1989).

6 **Fenyvesi, A.**, Mahunka, I., Tárkányi, F., Molnár, T., Béres, Cs., Kovács, Z., Mikecz, P., Szűcs, Z.
Production of ^{43}K and ^{24}Na radioisotopes in carrier-free form for use in radioecological studies at the forest area of the Síkfökút Project
In *Responses of Forest Ecosystems to Environmental Changes*. Eds.: Teller, A., Mathy, P., Jeffers, J.N.R., Elsevier Applied Science, London and New York, 1992, pp. 608-609.

7 Raschi, A., Tognietti, R., Ridder, H.-W., Béres, Cs., **Fenyvesi, A.**
The use of computer thomography in the study of pollution effects on oak trees
Agricoltura Mediterranea, Special Volume, Responses of Plants to Air Pollution, 298(1995).

8 Tognietti, R., Raschi, A., Béres, C., **Fenyvesi, A.**, Ridder, H.-W.
Comparison of sap flow, cavitation and water status of *Quercus petraea* **and** *Quercus cerris* **trees with special reference to computer tomography**
Plant, Cell and Environment **19**, 928 (1996).

9 **Fenyvesi, A.**, Béres, Cs., Ridder, H.-W., Raschi A., Molnár, T., Röfler, J., Lakatos, T. and Csiha, I.
Sap-flow velocities and distribution of wet-wood in trunks of healthy and unhealthy *Quercus robur*, *Quercus petraea* **and** *Quercus cerris* **oak trees in Hungary**
Chemosphere (in press).

Other publications, dealing with related technical developments:

10 **Fenyvesi, A.**, Mahunka, I., Molnár, T.
Status report on the fast neutron irradiation facility for radiobiological purposes at the Debrecen cyclotron
Zeitschrift für Medizinische Physik **1**, 30 (1991).

11 **Fenyvesi, A.**, Gál, I., Mahunka, I., Molnár, T., Tárkányi, F., Csejtei, A.
Nagyintenzitású ciklotron neutronforrások
Magyar Radiológia **63**, l66 (l989)
(High intensity cyclotron neutron sources
Hungarian Radiology **63**, 166 (l989)) (in Hungarian).

12 Molnár, T., **Fenyvesi, A.**, Mahunka, I., Csejtei, A.
Dozimetriai mérések nagyintenzitású ciklotron neutronforrásokon
Magyar Radiológia **63**, l59 (l989)
(Dosimetric measurements at high intensity cyclotron neutron sources
Hungarian Radiology **63**, l59 (l989)) (in Hungarian).

13 **Fenyvesi, A.**
Az MGC-20 ciklotronra alapozott gyorsneutron források és alkalmazásaik
Egyetemi doktori értekezés
Kossuth Lajos Tudományegyetem, Debrecen, 1990.
(Fast neutron sources based on the MGC-20E cyclotron and their applications
dr. univ. Thesis
Lajos Kossuth University, Debrecen, Hungary, 1990) (in Hungarian).

Contents

1. Introduction

The first motivation behind the present work was a request of the Department of Ecology of Lajos Kossuth University (Debrecen, Hungary) in 1987. They asked the Cyclotron Application Department of the Institute of Nuclear Research of the Hungarian Academy of Sciences (ATOMKI, Debrecen, Hungary) to develop a radioactive tracer technique and later to combine it with the thermometry method invented by Granier [1] to study the intensity of the sap-flow in healthy and unhealthy oak trees at the research forest area of the Síkfőkút Project of Lajos Kossuth University (Debrecen, Hungary). Some radioisotope of sodium or potassium in no-carrier-added form had to be considered as tracer to avoid any undesirable concentration effect. Radiation protection measures prescribed by the regional authorities for the planned field experiments lasting several days limited the choice of radioisotopes to ^{24}Na ($T_{1/2}$ = 14.96 h), ^{42}K ($T_{1/2}$ = 12.36 h) and ^{43}K ($T_{1/2}$ = 22.3 h) [2]. These isotopes are frequently used as tracers in various other types of studies, too. In long term studies need radioisotope of sodium, ^{22}Na ($T_{1/2}$ = 2.6 y) [2] is applied usually. ^{24}Na and ^{22}Na are widely used for calibration of nuclear measurement devices. The potential applications of these isotopes induced us to find possible routes of production of ^{22}Na, ^{24}Na, ^{42}K and ^{43}K at medium sized multiparticle accelerators ($E_p \leq 40$ MeV) and especially at the MGC-20E cyclotron of ATOMKI.

As a first step, we experimentally studied the possibilities of production of ^{24}Na via the ^{27}Al(n,α)^{24}Na reaction at the 18 MeV p(Be) intense fast neutron source at the MGC-20E cyclotron [3, 4, 5, 6]. Aluminium and Al_2O_3 powder were irradiated with neutrons [7,8]. The difficulties in the chemical separation of ^{24}Na underlined the necessity of finding other route(s) suitable for production of radioisotopes of sodium or potassium.

A survey of the literature and the EXFOR data base of the Nuclear Data Section of the International Atomic Energy Agency (IAEA, Vienna, Austria) showed that the excitation functions of proton, deuteron, ^{3}He- and α-particle induced reactions on neon isotopes are not well measured even below 20 MeV. The same was found for the ^{40}Ar(α,p)^{43}K reaction which is the most commonly used reaction for producing ^{43}K and it is the only one that fulfils the requirements of low energy cyclotrons. Additionally, no theoretical estimation of the excitation function of the ^{40}Ar(α,p)^{43}K reaction had been published before our work. Hodgson [9] and Avrigeanu *et al.* [10] emphasised that more cross section data would be valuable

also for studying the (α,p) reaction mechanism. Also, new cross section data would be useful to check, validate and/or improve the capabilities of nuclear reaction model codes.

Considering their Coulomb-barriers and Q-values, at least the $^{22}Ne(p,n)^{22}Na$, $^{20}Ne(d,\alpha)^{18}F$, $^{20}Ne(^{3}He,p)^{22}Na$ and $^{20}Ne(^{3}He,n)^{22}Mg\rightarrow^{22}Na$ reactions can have some astrophysical interest, too. The Coulomb-barrier for the $^{22}Ne(p,n)^{22}Na$ and $^{20}Ne(d,\alpha)^{18}F$ reactions is 2.7 MeV and 2.6 MeV, respectively, while it is 4.9 MeV for the $^{20}Ne(^{3}He,p)^{22}Na$ and $^{20}Ne(^{3}He,n)^{22}Mg\rightarrow^{22}Na$ reactions. The temperature in silicon burning stars having Ne-rich core or shell is some $4*10^{9}$ K (MeV). The estimated peak temperature in the supernova explosion of single silicon burning massive stars is $T > 4.5*10^{9}$ K [11]. No detailed study dealing with these processes in closed stellar systems has hitherto been reported [12] but in these cases the peak temperature in the shock wave in the supernova explosion of a silicon burning star might be even slightly higher. Taking into account the uncertainties of astrophysical model calculations, the reactions mentioned above might contribute to the explosive stellar nucleosynthesis. Measurement of new cross sections for the above reactions would be a contribution to the international activity to provide more complete nuclear data required for new generation of supernova models and codes [13].

As a summary, new excitation function measurements for proton, deuteron, ^{3}He- and α-particle induced nuclear processes on neon and for the $^{40}Ar(\alpha,p)^{43}K$ reaction would provide valuable information for nuclear physics, nuclear astrophysics as well as for optimisation of radionuclide production at low energy multiparticle cyclotrons for practical applications.

Chapter 2 of this thesis gives a short overview on the practical applications and production of ^{22}Na, ^{24}Na and ^{43}K radioisotopes and on the available relevant nuclear data. Chapter 3 summarises the basic assumptions of cross section and yield measurements via the activation method using gas targets. Chapter 4 presents the experimental techniques used and data resulted measuring by us the excitation functions of the $^{nat}Ne(d,x)^{18}F$, $^{nat}Ne(^{3}He,x)^{22,24}Na$, $^{nat}Ne(\alpha,x)^{22,24}Na$ processes and the $^{40}Ar(\alpha,p)\ ^{43}K$ reaction. Calculated and measured thick target yields are also presented. Chapter 5 describes the methods developed by us to produce significant amount of no-carrier added ^{24}Na and ^{43}K radioisotopes at a small multiparticle cyclotron. Chapter 6 presents some results obtained by us applying ^{24}Na and ^{43}K radioisotopes as tracers in studying the water transport in the trunks of mature oak trees. A reference list is also given at the end of the thesis.

2. Application and production of ^{22}Na, ^{24}Na and ^{43}K radioisotopes

2.1 Application of ^{22}Na, ^{24}Na and ^{43}K

A great number of specific applications of sodium and potassium radioisotopes ^{22}Na [$T_{1/2}$ = 2.60 y, Q_{ε} = 4788.1 keV, E_{γ} = 1274.5 keV (99.94 %)], ^{24}Na [$T_{1/2}$ = 14.96 h, Q_{β^-} = 5513.6 keV, E_{γ} = 1368.6 keV (100 %), 2754.0 keV (99.94 %)], ^{38}K [$T_{1/2}$ = 7.636 min, $Q_{\beta-}$ = 4.916 MeV, E_{γ} = 2.167 MeV (99.86 %)], ^{42}K [$T_{1/2}$ = 12.36 h, $Q_{\beta-}$ = 3.525 MeV, E_{γ} = 1.525 MeV (18.8 %)] and ^{43}K [$T_{1/2}$ = 22.3 h, $Q_{\beta-}$ = 1.817 MeV, E_{γ} = 220.58 keV (4.08 %), 372.81 keV (86.7 %), 396.93 keV (11.36 %), 593.39 keV (11.0 %), 617.51 keV (80.0%)] [2] have been documented, e.g. by the Integrated Nuclear Information System (INIS) of the International Atomic Energy Agency, Vienna, Austria.

^{22}Na and ^{24}Na radioisotopes have been used as tracers in studying flow patterns as well as velocity and flow rates of fluids (e. g. melted glass in furnaces, depositions in sewage pools, water in living organisms, etc.), and/or retention times of solvents or components of mixtures traversing irregularly shaped storage volumes (e. g. cells, organs, flotation cells, digesters, cokers, bleaching towers, soils, etc.). ^{22}Na and ^{24}Na are widely used for calibration of nuclear measurement devices. ^{22}Na has recently also been suggested for use in calibration of PET cameras [14]. The presence of Na-carrier is not a problem in most of the applications. Nevertheless, the no-carrier-added form of sodium radioisotopes is of advantage in microbiological experiments when the initial sodium uptake rate of cells at zero extracellular initial sodium concentration is studied [15].

Of radioisotopes of potassium, ^{43}K has the longest half life making it the most practical for use in experiments lasting several days in various types of biomedical and plant physiological studies. Most of the published biomedical applications of ^{43}K are for *in vivo* use in humans. ^{43}K has been utilised for myocardial function studies [16, 17, 18], ischaemia studies [19] and for many cardiovascular studies [20]. There have been examples of the application of ^{43}K for studying the electrolyte distribution and exchangeable potassium in the human body [21, 22, 23, 24, 25] and for body space and potassium transport measurements [26, 27]. It has also been used for studies concerning transport mechanisms in cell membranes [28].

2.2 Routes for production of ^{22}Na and ^{24}Na

^{22}Na and ^{24}Na are produced most frequently via neutron induced reactions on Na, Mg and Al at nuclear reactors. On the isotopes of these target elements, the following neutron induced reaction channels are opened for $E_n \leq 20$ MeV: ^{23}Na(n,2n)^{22}Na (Q = -12.42 MeV, E_{th} = 12.96 MeV), ^{23}Na(n,γ)^{24}Na (Q = 6.96 MeV), ^{24}Mg(n,p)^{24}Na (Q = - 4.73 MeV, E_{th} = 4.93 MeV), ^{25}Mg(n,d)^{24}Na (Q = - 9.84 MeV, E_{th} = 10.24 MeV), ^{25}Mg(n,pn)^{24}Na (Q = - 12.1 MeV, E_{th} = 12.55 MeV) and ^{27}Al(n,α)^{24}Na (Q = - 3.13 MeV, E_{th} = 3.25 MeV). Many experimental and evaluated data can be found in the different nuclear data libraries (e. g. CSISRS and ENDF) for these reactions illustrating that they are quite well measured.

Several charged particle induced reactions lead to the formation of ^{22}Na and ^{24}Na. At this time the EXFOR data base of the Nuclear Data Section of the International Atomic Energy Agency (IAEA, Vienna, Austria) seems to be the most complete source of measured and calculated nuclear data for these reactions. A comprehensive collection of available experimental excitation function data can be found in [29] and [30] for proton, deuteron, ^{3}He- and α-particle induced reactions at low and intermediate projectile energies. Calculated integral yields in tabulated form are listed for many reactions by Dmitrijev [31].

The problems of targetry and chemical separation of the product can be solved relatively easily in the cases of employing proton, deuteron, ^{3}He- and α-particle induced processes on isotopes of F, Ne, Na, Mg and Al leading to the formation of ^{22}Na and ^{24}Na. These routes can be suitable for producing ^{22}Na and ^{24}Na with yield of 10^{-1} kBq/μAh or higher below 40 MeV incident charged particle energy considering their Q-values and the available excitation function data (Table 2-1.).

2.3 Production of ^{18}F, ^{22}Na and ^{24}Na on isotopes of Neon

Not only ^{22}Na and ^{24}Na but the positron emitter radioisotope ^{18}F can be produced via nuclear reactions induced by proton, deuteron, ^{3}He- and α-particles on isotopes of Neon. ^{18}F is widely used for nuclear medicine especially for Positron Emission Tomograpy (PET) studies. Despite of this fact, only a few cross section data have been published on these processes.

Reddy *et al.* [32] measured cross sections of the ^{20}Ne(p,p2n)^{18}Ne → ^{18}F and ^{20}Ne(p,2pn)^{18}F reactions in the energy range 25 MeV ≤ E_p ≤ 100 MeV.

Table 2-1. A comprehensive list of literature relevant to the production of ^{22}Na and ^{24}Na via proton, deuteron, ^{3}He- and α-particle induced nuclear reactions on isotopes of F, Na, Mg and Al.

Product	Route	Reference
^{22}Na	^{19}F(α,n)	Albert *et al.* [29] Norman *et al.* [33]
	^{23}Na(p,x)	Iljonov *et al.* [30]
	^{23}Na(d,x)	Bowen *et al.* [34] Lange *et al.* [35]
	^{nat}Mg(p,x)	Iljonov *et al.* [30]
	^{25}Mg(p,α)	Meadows *et al.* [36] Cohen *et al.* [37]
	^{nat}Mg(d,x)	Dmitrijev [31]
	^{27}Al(p,x)	Bodemann *et al.* [38]
	^{27}Al(d,x)	Michel *et al.* [39] Martens *et al.* [40]
	^{27}Al(^{3}He,x)	Cochran *et al.* [41] Brill [42] Lamb [43] Michel *et al.* [39]
	^{27}Al(α,x)	Martens *et al.* [40]
^{24}Na	^{23}Na(d,p)	Bowen *et al.* [34] Lange *et al.* [35]
	^{nat}Mg(p,x)	Wilson *et al.* [44]
	^{nat}Mg(α,x)	Cohen *et al.* [45] Meadows *et al.* [46]
	^{nat}Mg(d,x)	Wilson *et al.* [44] Bartell *et al.* [47]
	^{26}Mg(d,α)	Rohm *et al.* [48]
	^{nat}Mg(α,x)	Frantsvog *et al.* [49]
	^{27}Al(p,x)	Hintz *et al* [50] Cumming [51] Miyano [52] Holub *et al.* [53] Grütter [54] Schneider *et al.* [55]
	^{27}Al(d,x)	Weinreich *et al.* [56] Michel *et al.* [39] Martens *et al.* [40 Rohm *et al.* [48]
	^{27}Al(^{3}He,x)	Weinreich *et al.* [56] Cochran *et al.* [41] Brill [42] Lamb [43]
	^{27}Al(α,x)	Martens *et al.* [40] Lindsay *et al.* [57] Michel *et al.* [58]

Ruth [59] reported a method for production of ^{18}F via the $^{20}Ne(p,x)^{18}F$ process. The $^{22}Ne(p,n)^{22}Na$ reaction was investigated by Saam *et al.* [60] and recently, in more details, Takács *et al.* [14] the energy range 5 MeV $\leq E_p \leq$ 18 MeV.

Nuclear data for the $^{20}Ne(d,\alpha)^{18}F$ reaction and the $^{20}Ne(d,x)$ processes are also rather scarce although the $^{20}Ne(d,\alpha)^{18}F$ reaction is widely used for production of ^{18}F labelled F_2 gas for nuclear medicine purposes. Guillaume [61] and Nozaki *et al.* [62] published only excitation curves for the $^{20}Ne(d,\alpha)^{18}F$ reaction in the energy range from threshold up to 15 MeV. Experimental errors were not published by them. Backhausen *et al.* [63] published measured cross sections in the energy region of 20 MeV $\leq E_d \leq$ 50 MeV for these reactions. Targetry solutions and measured thick target yields were published by Lagunas-Solar and Carvacho [64] and Helus *et al.* [65].

Experimental studies done on ^{nat}Ne at Jülich [63, 66, 67], i. e. $^{nat}Ne(^3He,x)$ and $^{nat}Ne(\alpha,x)$ processes, dealt only with the production of ^7Be, ^{18}F and ^{18}Ne. For the $^{nat}Ne(\alpha,x)^{22}Na$ process only the thick target yield was measured at E_α = 27 MeV [68]. The $^{nat}Ne(^3He,x)^{22,24}Na$ processes have not been investigated experimentally.

2.4 *Routes for production of ^{43}K*

Numerous papers have been published on the detection of ^{43}K as product in alpha, ^{12}C and some other heavy ion induced nuclear reactions (see e.g. the EXFOR data base of the Nuclear Data Section of the IAEA, Vienna). Only some of the numerous possible routes are of practical importance and have been used for the production of ^{43}K for labelling purposes: $^{40}Ar(\alpha,p)$ [69, 70, 71, 72], $^{44}Ca(\gamma,p)$ [73, 74], $^{43}Ca(n,p)$ [75], $^{nat}V(p,spall)$ [20, 76, 77, 78] and $^{51}V(d,2\alpha pn)$ [79]. Although the $^{40}Ar(\alpha,p)^{43}K$ reaction is the most commonly used one for producing ^{43}K, only a few data points for its excitation function have been measured (Tanaka *et al.* [80]). Data for the thick target yield published by different groups also show large deviations.

In order to achieve an efficient production and recovery procedure for ^{43}K produced via the $^{40}Ar(\alpha,p)$ reaction, different technical solutions have been developed in different laboratories. In most cases high-volume-low pressure targets, used in batch mode, were employed. The produced activity was collected by rinsing

an internal collecting electrode [69] or an internally inserted rotating liner [61] or the target chamber wall by a steaming method [81].

Studies of the penetration of bombarding beams in gas targets have shown a significant density reduction in the bombarded volume of the gas, which results a low production yield and undesirable activation of the target chamber. The density reduction can be minimised by avoiding dead volumes surrounding the beam strike region, using a small volume and high pressure target [82]. Another advantage of a small volume chamber is that it allows the collection of the activity in a smaller volume of rinsing solvent [72]. However, the high pressure targets require thicker windows and better cooling conditions. Recently Tárkányi *et al.* [83] investigated the static and dynamic effects in targets containing Neon or Argon gas and irradiated by α-particles. They used an optical method and they studied alterations of the density reduction at different beam intensities and pressures.

An alternative way to avoid the complicated and ineffective recovery of the ^{43}K activity produced in a large volume target and to reduce the radiation hazard during the recovery procedure is to use the continuous flow mode for flushing the argon and the product nuclei out of the target volume. The activity can be collected on an external filter from which it can easily be removed by washing [70, 71]. However, a decreasing recovery yield has been observed over long time periods due to the increasing adsorption of the potassium by the aluminium target walls [81].

3. Basic assumptions of cross section and yield measurements via the activation method using gas targets

3.1 Cross section measurements

The change of density of active nuclei produced by a nuclear reaction of type I(i,j)J at a point P in an irradiated target is

$$dn_J(\vec{r}_P;t)=\left(\frac{\rho_I(\vec{r}_P;t)dV}{M_I}N_A g_c g_{is}\int_0^{E_{i;\max}}\varphi_i(\vec{r}_P;t;E_i)\sigma(E_i)dE_i-\lambda_J n_J(\vec{r}_P;t)\right)dt \qquad (3.1)$$

The meaning of symbols in (3.1) are:

n_J	density of product nuclei,
$\vec{r}_P$	position vector of the point P,
t	time
ρ_I	density of target nuclei,
dV	an infinitesimally small volume around the point P,
M_I	molar mass of the target material,
N_A	the Avogadro number,
g_c	chemical abundance of the target element in the matrix,
g_{is}	isotopic abundance of the target nuclei,
φ_i,E_i	flux and energy of the bombarding particles, respectively,
$\sigma(E_i)$	excitation function of the I(i,j)J nuclear reaction,
λ_J	decay constant of the radioactive isotope to be produced.

The activity is defined as $A_J(t)\equiv\lambda_J n_J(t)$. The determination of the excitation function $\sigma(E_i)$ on the basis of equation (3.1) is the same problem, mathematically, than the problem of neutron spectrum unfolding from a set of measured reaction rates and well known excitation functions in neutron physics. The sophisticated unfolding of $\sigma(E_i)$ could be performed if the $n_J(\vec{r}_P;t)$, $\rho_I(\vec{r}_P;t)$ distributions and a set of $\varphi_i(\vec{r}_P;t;E_i)$ and the necessary covariance information would be available.

In practice, the irradiation conditions enable a simpler way of determination of $\sigma(E_i)$. Typically the incident charged particle beam is "quasi monoenergetic" and its divergence is small. Inhomogenity of the current density distribution is supposed to be small. It can be ensured by appropriate beam transportation. Especially in the cases of gas targets, low currents are used to keep the density reduction negligible and then ρ is considered to be constant and homogenous in the irradiated volume. At these circumstances the problem (3.1) can be reduced to a 1-dimensional one and $\varphi(\vec{r}_P;t;E_i)$ can be written in the following form:

$$\varphi\left(x;t;E_{i;0};E_i;E_{i;x}\right)=\frac{I_i(t)}{z_i e\left(d/2\right)^2\pi}*\psi\left(E_{i;0};E_i\right)*\chi\left(E_i;E_{i;x};x\right) \qquad (3.2)$$

where

x	is the depth in the target,
$E_{i;0}$	is the average energy of the bombarding particles of i on the surface of the target,
$E_{i;x}$	is the energy of the particle i at the depth x in the target,
$I_i(t)$	is the current of the bombarding beam at the instant t,
z_i	is the atomic number of the bombarding particles,
e	is the elementary charge of electron,
d	is the diameter of the bombarding beam,
$\psi(E_{i;0};E_i)$	is the probability density for the incident particles at the surface of the target to have an energy E_i,
$\chi(E_i;E_{i;x};x)$	is the probability density for the i particle of energy E_i at the surface of the target to have a reaction energy $E_{i;x}$ at a depth x.

The distribution $\psi(E_{i;0};E_i)$ is approximately Gaussian with a parameter δ_b:

$$\psi\left(E_{i;0};E_i\right)=\frac{1}{\sqrt{2\pi\delta_b{}^2}}e^{-\frac{\left(E_i-E_{i;0}\right)^2}{2\delta_b{}^2}}. \qquad (3.3)$$

The $\chi(E_i;E_{i;x};x)$ describes the straggling effects and it can be estimated using the Vavilov-Landau theory (see e. g. [84]). For large penetration depth, the distribution of the energy loss is approximately Gaussian:

$$\chi\left(E_i; E_{i;x}; x\right) = \frac{1}{1.06\Gamma} e^{-\frac{\left(\left(E_i - E_{i;x}\right) - \left(E_i - E_{i;x}\right)_0\right)^2}{0.36\Gamma^2}}$$

(3.4)

and

$$\Gamma = 0.93 z_i \left(\frac{\overline{Z}_I}{\overline{A}_I} x\right)^{1/2} \text{(MeV)}$$

(3.5)

where

$(E_i - E_{i;x})_0$	denotes the mean energy loss corresponding to the depth x,
$\overline{Z}_I$	is the average atomic number of the target,
$\overline{A}_I$	is the average mass number of the target.

The relation between x and $(E_i - E_{i;x})_0$ is the following:

$$x = \int_{E_i - (E_i - E_{i;x})_0}^{E_i} \frac{dE_i}{S(E_i)}$$

(3.6)

where $S(E_i)$ is the stopping power for the i particles as a function of energy. After these considerations (3.1) can be written in the following form:

$$\frac{dn_J}{dt} + \lambda_J n_J = \frac{\rho_I N_A g_c g_{is} (d/2)^2}{M_I} * \frac{I(t)}{z_i e (d/2)^2} * \int_{x=0}^{D} \int_{E_i=0}^{\infty} \int_{E_{i;x}=0}^{\infty} \psi_i\left(E_{i;0}; E_i\right) \chi_i\left(E_i; E_{i;x}\right) \sigma(E_i) dE_{i;x} dE_i dx$$

(3.7)

where D is the thickness of the target. For $t = \infty$, the formation and the decay of nuclei of type J are in equilibrium at a constant current I. Then $dn_J/dt = 0$ and

$$A_{J;sat} \equiv \lambda_J n_J(\infty) = \frac{\rho_I N_A g_c g_{is} I}{M_I z_i e} * \int_{x=0}^{D} \int_{E_i=0}^{\infty} \int_{E_{i;x}=0}^{\infty} \psi_i\left(E_{i;0}; E_i\right) \chi_i\left(E_i; E_{i;x}\right) \sigma(E_i) dE_{i;x} dE_i dx$$

(3.8)

where $A_{J;sat}$ is the saturation activity. For a specific average incident energy $E_{i;0}$, in practice, only an averaged value of the cross section is determined from the measurements. It is defined as

$$<\sigma(E_{i;0})> \equiv \frac{\int_{x=0}^{D}\int_{E_i=0}^{\infty}\int_{E_{i;x}=0}^{\infty}\psi_i(E_{i;0};E_i)\chi_i(E_i;E_{i;x})\sigma(E_i)dE_{i;x}dE_i dx}{\int_{x=0}^{D}\int_{E_i=0}^{\infty}\int_{E_{i;x}=0}^{\infty}\psi_i(E_{i;0};E_i)\chi_i(E_i;E_{i;x})dE_{i;x}dE_i dx}.$$

(3.9)

It can be supposed that the total flux of the charged particle beam is the same before and behind the target because the small cross section of nuclear reactions. Then the relationship between the activity of the target at the end of irradiation (**E**nd **O**f **B**ombardment) $A_{J;EOB}$ and the average cross section $<\sigma>$ can be written as

$$A_{J;EOB} = \frac{\rho_I N_A g_c g_{is} D}{M_I z_i e} * H^* <\sigma>$$

(3.10)

where

$$H = \sum_{k=1}^{n}\left[I_k * \left(1 - \exp\left(-\lambda_J\left(t_k - t_{k-1}\right)\right)\right) * \exp\left(-\lambda_J\left(t_{EOB} - t_k\right)\right)\right].$$

(3.11)

The averaged cross section $<\sigma>$ can be calculated by the following way

$$<\sigma> = \frac{M_I z_i e}{\rho_I N_A g_c g_{is} D H} * A_{J;EOB}.$$

(3.12)

The EOB activity $A_{J;EOB}$ can be calculated from the counts detected by the measuring system and corrected for the background. In the case of employing gamma spectrometry,

$$A_{J;EOB} = \frac{\lambda_J C}{\exp\left(-\lambda_J t_c\right) * \left(1 - \exp\left(-\lambda_J t_m\right)\right) * \varepsilon_{corr}}$$

(3.13)

where

C is the net area of one of the relevant full energy photo peak,

t_c is the time elapsed from the end of the irradiation to the start of the activity measurement

t_m is the real time of the measurement.

The factor ε_{corr} in (3.13) includes corrections for different losses:

$$\varepsilon_{corr} = \varepsilon_b * \varepsilon_c * \varepsilon_\gamma * \frac{t_{LIVE}}{t_m} \qquad (3.14)$$

where

ε_b is the ratio of decays result the gamma line to be counted,

ε_c is the correction for random and true coincidences,

ε_γ is the detection efficiency for the full energy gamma peak to be counted

t_{LIVE} is the live time of the measurement provided by the measuring system.

The energy of incident particles can be high enough to open other reaction channels (e.g. break up of the outgoing particles) producing nuclei of J-type. A cumulative cross section is measured by the activation method in this case. Moreover, in many practical cases, some of the other isotopes of the target element also contribute to the formation of J-type nuclei and then cumulated elemental cross sections are resulted. Equations of this chapter can be generalised easily for these cases.

3.2 Yields

The yield achievable using a homogenous target of thickness D is

$$Y(D;E_{i;0}) \equiv \frac{\rho_I N_A g_c g_{is}}{M_I} * \int_{x=0}^{D} \int_{E_i=0}^{\infty} \int_{E_{i;x}=0}^{\infty} \psi_i(E_{i;0};E_i)\chi_i(E_i;E_{i;x})\sigma(E_i)dE_{i;x}dE_i dx \,. \qquad (3.15)$$

If D is higher than the maximal range of the bombarding particles in the target then the $Y(D;E_{i;0})$ is called thick target yield. The integral yield of the I(i,j)J reaction is defined as

$$Y\left(E_{i;0}\right) \equiv \frac{\rho_I \, N_A \, g_c \, g_{is}}{M_I} * \int_{E_i=0}^{E_i=E_{i;0}} \frac{\sigma\left(E_i\right)}{S\left(E_i\right)} dE_i \, .$$

(3.16)

Obviously, it is valid that $Y(D;E_{i;0}) \leq Y(E_{i;0})$.

The left side of Eq. (3.7) is used to define other yields used in the practice of radioisotope production [85]. They are derived from values of $A_J(t)$ measured at specific instants i.e. at the **E**nd **O**f an **I**nstantaneous **B**ombardment (EOIB) or after **1 h** or at the **E**nd **O**f **B**ombardment (EOB). They are defined for both infinitesimally thin and thick targets. Theoretically they could be calculated as the time integrals of the right side of Eq. (3.7) using the relevant target thicknesses. In practice, $\psi(E_{i;0};E_i)$, $\chi(E_i;E_{i;x})$ and, in gas targets, the density distribution are not known exactly.

4. Excitation functions of the $^{nat}Ne(d,x)^{18}F$, $^{nat}Ne(^3He,x)^{22,24}Na$, $^{nat}Ne(\alpha,x)^{22,24}Na$ processes and the $^{40}Ar(\alpha,p)^{43}K$ reaction

We have measured cross sections of the $^{nat}Ne(d,x)^{18}F$, $^{nat}Ne(^3He,x)^{22,24}Na$, $^{nat}Ne(\alpha,x)^{22,24}Na$ processes and the $^{40}Ar(\alpha,p)^{43}K$ reactions at various energies of incident particle. This chapter includes a brief summary of experimental techniques used and results of excitation function measurements presented by us in Papers 1-4 [86, 87, 88, 89].

4.1 The experimental technique

Irradiations were carried out at the external beam of the MGC-20E cyclotron at ATOMKI (Debrecen) [90] and the CV 28 compact cyclotron at Institut für Nuklearchemie, Forschungszentrum Jülich GmbH (Jülich. Germany).

Excitation functions were measured by the activation method using single and stacked gas cell targets. The experimental techniques were similar or identical to those described in more detail in several earlier publications from Jülich and Debrecen [cf. Refs. 14, 63, 66, 67, 91, 92].

Stainless steel cells (2 cm dia, 2.5 cm length) having windows of different thicknesses (10 μm Ti, 22 μm Ti, 25 μm Ag or 50 μm Al) were filled with the target gas (technical purity argon or 99.99 % purity neon gas) up to 100 - 300 kPa (1 - 3 bar) using the gas handling and pressure measuring system described in Ref. [92]. Collimated beams (dia ≤ 5 mm) were used and at most three cells were stacked together to contain the whole broadened beam within the targets [91]. In the case of measuring the excitation function of the $^{nat}Ne(^3He,x)^{22}Na$ process, several experiments were conducted using gas cells with a cylindrical internal aluminium liner inserted in each of them. This allowed an easy removal of the produced activity from the cell [cf. Refs. 66, 67].

The energies of the primary beams were determined via deflection in a calibrated magnetic field at the Debrecen cyclotron [93] and by measuring the separation between neighbouring bunches in the beam transport line at the CV 28 cyclotron in Jülich [94].

Aluminium, titanium and copper foils were used to degrade the beam energy to the desired value and to monitor the intensity and the energy of the bombarding beam. The windows of the gas target cells served as monitor foil, as well, in many cases.

The number of bombarding particles was determined both from direct beam current measurement via electric charge collection in a Faraday cup and by monitor reactions. The ^{nat}Ti(d,x)^{48}V [95] and the ^{nat}Ti(^{3}He,x)^{48}V reactions [56, 96] were used for monitoring the intensity and the energy of the deuteron and ^{3}He particles over the whole energy range. Above 15 MeV, the ^{27}Al(^{3}He,x)^{22}Na reaction [39, 41, 42, 43] induced in separate monitor foils was also used. Alpha particle beams were monitored via the ^{nat}Ti(α,x)^{51}Cr, [56, 96] and ^{nat}Cu(α,x)^{66}Ga [96]. The flux values obtained via different monitor reactions at a given energy point agreed within 5 %. The maximum deviations between the flux values obtained via monitor reactions and Faraday-cup measurements were approximately 20 % at the first cells and some 30 % at the last cells. The average of flux values obtained from the monitor reactions was used for cross section calculations.

Irradiations were done at beam currents ≤ 500 nA to minimise the density reduction of the target gas.

4.1.1 Treatment of targets after irradiation and activity measurements

^{nat}Ne(^{3}He,x)^{22,24}Na, ^{nat}Ne(α,x)^{22,24}Na and ^{40}Ar(α,p)^{43}K

In the most cases, using Ti windows, the produced activity could be determined without removing the gas from the irradiated cell.

In some experiments done in Jülich using Ti windows and neon gas as target material, the produced ^{22,24}Na activity was removed from the cell by rinsing with solution containing carrier (for details see Paper 3 [86]) and the extent of activity removal was investigated via counting separately the liquid fraction and the target chamber containing some residual activity. The production of ^{22,24}Na in the windows was also checked by this way and it was found to be negligible.

The primary aim of experiments done in Jülich using Al and Ag windows and liners was the determination of the excitation function of the ^{nat}Ne(^{3}He,x)^{7}Be

process. However, the treatment of gas cells and the method of radiochemical separation of ^{7}Be (for details see Refs. [66, 67]) enabled the quantitative measurement of the amount of ^{22}Na produced, too. In the case of Al windows, a significant correction was necessary for the ^{22}Na activity formed in the windows (for details see Paper 3 [86]). A fitted average of the experimental excitation functions reported in the literature [cf. Refs. 39, 41, 42, 43] was used for this correction.

The activities were measured using high-resolution gamma-ray spectroscopy (i.e. HPGe detectors with the necessary electronics, PC multichannel analyzer cards and spectrum evaluation softwares). Counting was done at large detector-source distances to keep low the pile up and coincidence losses and to avoid calibration problems for extended sources.

$^{nat}Ne(d,x)^{18}F$

In the case of investigating the excitation function of the ^{nat}Ne(d,x)^{18}F nuclear reaction, the activity of the positron emitting ^{18}F was determined by gamma spectrometry using a HPGe detector. The counting was done at large source-detector distances. Decay curves were measured to identify the half-life of ^{18}F isotope. The two ends of the irradiated gas cells were covered by aluminium disks of 1 mm thickness while counting the 511 keV annihilation peak of the gamma spectrum. The coverage ensured the localisation of the annihilation of positrons within the sample area. It was checked by positron emission tomography at the PET camera of the PET Centre of the University Medical School of Debrecen. Tomograms of both the uncovered and covered irradiated target were taken. A standard ^{22}Na source was used to determine the detection efficiency for the actual geometry.

4.2 Determination of the mean energies

The energy loss of the bombarding beam was determined by calculation using data and methods in Refs. [97, 98]. Monitor foils were also applied to evaluate the actual target thicknesses.

The mean energy of the beam at the middle of the irradiated cell and the monitor foil was computed as described earlier [cf. Refs. 99, 100]. It was also used for the determination of the target thickness. This was done by measuring the induced activity in the foils and comparing them to the activities estimated

from the calculated energy loss along the stack via the computation method described in Ref. [99].

4.3 Error estimations

The total error of cross sections was obtained by summing in quadrature the relative errors of the factors encountered in the determination of the cross sections: determination of the disintegration rate (statistical error and peak area analysis 1-20 %, detector efficiency 5 %, decay data 3 %, aliquotization of rinse solution 10 %); the number of target nuclei (target pressure 5 %, membrane effect of the target window 3 %, density reduction by beam heating 5 %) and the particle intensity 8 %.

The total error in the energy of each cross section point was also estimated. Uncertainties in the primary energies of the incident particles, the tabulated values of the range - energy relationships, the foil thicknesses, the gas pressures and beam energy straggling were taken into account in the error estimation.

Some other additional sources of errors had to be considered in the cases of the $^{nat}Ne(^{3}He,x)^{22,24}Na$ and $^{nat}Ne(\alpha,x)^{22,24}Na$ processes. Stacks of gas cells with Al windows were irradiated in some experiments. At energies above 14 MeV the contribution from aluminium windows to ^{22}Na formation is comparable to the total activity. The error involved in the estimation of the correction for the activity produced in the aluminium windows was also considered. It gives the main contribution to the total error of data obtained using gas cells filled up to 1 bar. Special corrections were necessary in effective target thickness and beam flux for the points below 5 MeV since part of the beam either was stopped inside the target gas or its energy was below the Coulomb barrier (4.7 - 5.0 MeV). The uncertainties both in the cross section and the energy scale of the points below 5 MeV are therefore inherently larger than those of the higher energy points.

4.4 Experimental excitation functions

The cross section data measured by us for the $^{nat}Ne(d,x)^{18}F$, $^{nat}Ne(^{3}He,x)^{22,24}Na$, $^{nat}Ne(\alpha,x)^{22,24}Na$ processes and for the $^{20}Ne(d,\alpha)^{18}F$ and $^{40}Ar(\alpha,p)^{43}K$ reactions and their uncertainties for various projectile energies are presented in Table 4-1 -Table 4-4 and Figure 4.1 - Figure 4.6. The energy

uncertainties are the FWHM values of the calculated energy distributions of the bombarding particles. The cross section uncertainties are for 1σ values.

The data presented for ^{nat}Ne are elemental cross sections, i.e. they describe the formation cross sections of activation products assuming neon to be monoisotopic. They include the contribution of all nuclear reactions leading directly, or through possible decay processes of some intermediate nuclei, to the formation of the products under investigation. ^{22}Na, for example, is produced directly in nuclear reactions as well as via the decay of the 3.6 s ^{22}Mg. ^{24}Na, on the other hand, is produced only by a combination of several nuclear reactions.

^{nat}Ne(d,x)^{18}F and ^{20}Ne(d,α)^{18}F

The ^{20}Ne(d,α)^{18}F (Q = 2.79 MeV) reaction is the only contributing reaction below E_d = 4.35 MeV. The threshold energy of the ^{21}Ne(d,αn)^{18}F (Q = - 3.97 MeV) reaction is E_{th} = 4.35 MeV. Above E_{th} = 15.64 MeV the ^{22}Ne(d,α2n)^{18}F (Q = - 14.33 MeV) also contributes to the formation of ^{18}F. Below 7.2 MeV our data are in good agreement with the curve published without experimental errors by Nozaki *et al.* [62]. It can be concluded that new data are needed to clear the discrepancies above 7.2 MeV.

Error! Not a valid link.

Figure 4.1. Excitation function of the ^{nat}Ne(d,x)^{18}F process (Paper 4 [87]).

Table 4-1. Measured cross sections of the ^{nat}Ne(d,x)^{18}F process [87].

Energy (MeV)	σ (mb)
2.8 ± 0.4	126.0 ± 16.9
3.9 ± 0.5	180.7 ± 24.3
4.6 ± 0.3	201.8 ± 27.1
6.2 ± 0.3	222.6 ± 29.9
6.8 ± 0.3	195.8 ± 26.3
7.2 ± 0.3	173.3 ± 23.3
8.5 ± 0.3	163.5 ± 22.0

^{nat}Ne(^{3}He,x)^{22}Na

Cross sections and the excitation function of the $^{nat}Ne(^{3}He,x)^{22}Na$ process measured by us are given in Table 4-2 and Figure 4.2, respectively. These are the first published excitation function data for this process as far as we know. The formation of ^{22}Na starts at low energies and reaches a maximum of some 140 mb at about 5 MeV. The main contributing processes at low energies are the $^{20}Ne(^{3}He,p)^{22}Na$ and $^{20}Ne(^{3}He,n)^{22}Mg \rightarrow {}^{22}Na$ reactions on the highly abundant target isotope ^{20}Ne(90.51 %). The long tail of the excitation function and especially some enhancement in the cross section at energies above 25 MeV are possibly due to contributions from direct interactions as well as from reactions with higher thresholds on the less abundant ^{21}Ne(0.27 %) and ^{22}Ne(9.22 %) target nuclei.

$^{nat}Ne(^{3}He,x)^{24}Na$

The excitation function of the $^{nat}Ne(^{3}He,x)^{24}Na$ process is given in Figure 4.3. Cross sections obtained are given also in Table 4-2. No other cross section data was found for this process in the literature. The formation of ^{24}Na also starts at very low energies and has a maximum value of some 4 mb at about 5 MeV. It is produced exclusively via the $^{22}Ne(^{3}He,p)^{24}Na$ reaction. The pure isotopic cross sections can therefore be obtained by normalisation of the elemental values to 100 % abundance of ^{22}Ne. The increase in the cross section at energies above 20 MeV is attributed to direct interactions. Since all the data were obtained using Ti windows, the contribution of the $^{27}Al(n,\alpha)^{24}Na$ reaction induced by secondary neutrons can be excluded. Presumably at high projectile energies an increased population of some very high lying energy levels of ^{25}Mg occurs. Those levels are unstable against proton decay [cf. Ref. 101], thus leading to an enhanced formation of the nucleus ^{24}Na.

Table 4-2. Measured cross sections of the $^{nat}Ne(^{3}He,x)^{22,24}Na$ processes (from Paper 3 [86]).

	$^{nat}Ne(^{3}He,x)^{22}Na$	**$^{nat}Ne(^{3}He,x)^{24}Na$**
Energy (MeV)	**σ (mb)**	**σ (mb)**
1.5 (-1.5, +2.0)	74.5 ± 59.6	2.7 (-2.2, +1.7)
2.0 (-2.0, +2.4)	2.4 (-2.4, +9.5)	0.0 (-0, +2)
2.8 (-2.8, +3.2)	103.5 ± 62.1	3.3 (-2.0, +1.2)
5.7 ± 2.2	132.1± 17.8	3.6 ± 0.8
5.9 ± 2.3	148.7 ± 23.3	4.5 ± 0.9
9.7 ± 1.7	73.5 ± 10.6	2.0 ± 0.4

10.4 ± 1.4	77.3 ± 13.2	
10.7 ± 1.5	79.8 ± 12.2	3.1 ± 0.7
11.6 ± 1.5	53.5± 8.2	1.6 ± 0.3
11.7 ± 1.6	48.2 ± 8.1	0.8 ± 0.2
12.7 ± 1.3	59.7 ± 11.0	1.8 ± 0.4
13.4 ± 1.6	59.5 ± 10.0	
14.1 ± 1.2	56.8 ± 9.4	1.4 ± 0.3
14.4 ± 1.3	56.3 ± 12.9	
15.5 ± 1.4	60.1 ± 10.2	
16.5 ± 1.1	22.0 ± 4.3	1.0 ± 0.2
17.6 ± 1.0	15.8 ± 6.4	0.4 ± 0.1
17.6 ± 1.2	30.8 ± 5.2	0.4 ± 0.1
18.3 ± 1.2	34.5 ± 6.9	
18.7 ± 0.8	29.0 ± 5.5	
19.4 ± 1.3	37.6 ± 6.3	1.1 ± 0.3
20.0 ± 1.0	27.3 ± 5.5	
22.2± 0.9	24.4 ± 20.4	
22.4 ± 0.9	24.2 ± 5.7	
22.5 ± 0.9	23.1± 3.9	0.6 ± 0.1
23.7 ± 1.5	32.9 ± 5.5	1.7 ± 0.4
23.9 ± 0.9	29.0 ± 4.9	0.7 ± 0.2
26.2 ± 1.3	28.9 ± 4.9	1.4 ± 0.3
27.7 ± 1.2	31.1 ± 5.2	2.0 ± 0.5
28.1 ± 0.8	48.9 ± 19.1	
29.9 ± 1.0	29.2 ± 4.9	1.4 ± 0.3
30.0 ± 0.6	9.6 ± 1.8	
30.3 ± 0.5	30.8 ± 15.6	
31.3 ± 0.9	33.6 ± 5.7	2.4 ± 0.5
33.3 ± 0.7	25.9 ± 4.4	2.2 ± 0.5

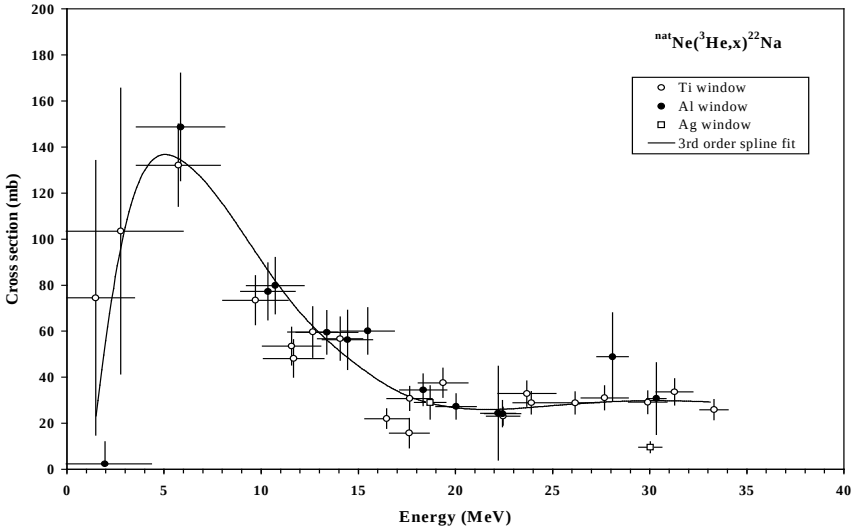

Figure 4.2. Measured excitation function of the $^{nat}Ne(^{3}He,x)^{22}Na$ nuclear process (from Paper 3 [86]).

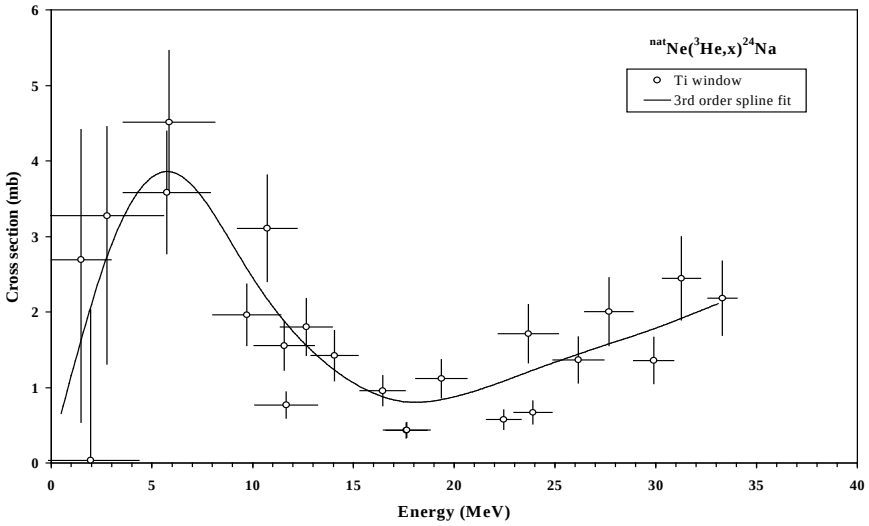

Figure 4.3. Measured excitation function of the $^{nat}Ne(^{3}He,x)^{24}Na$ nuclear process (from Paper 3 [86]).

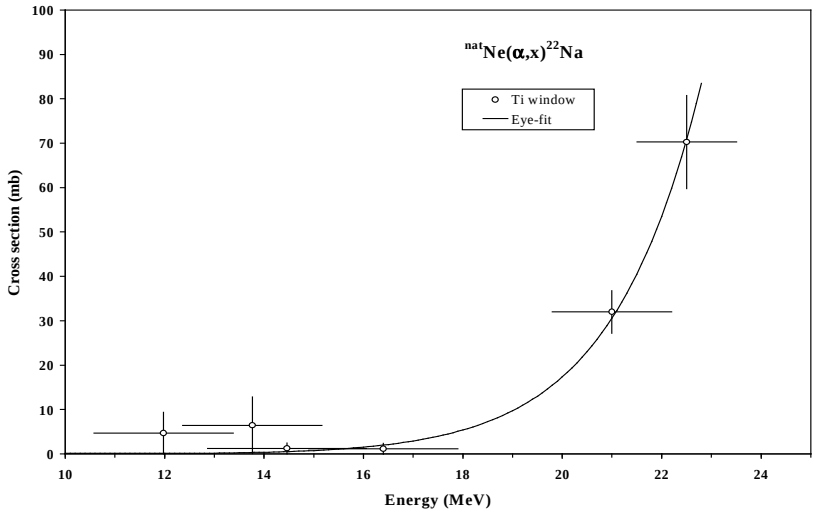

Figure 4.4. Measured excitation function of the ^{nat}Ne(α,x)^{22}Na nuclear process (from Paper 3 [86]).

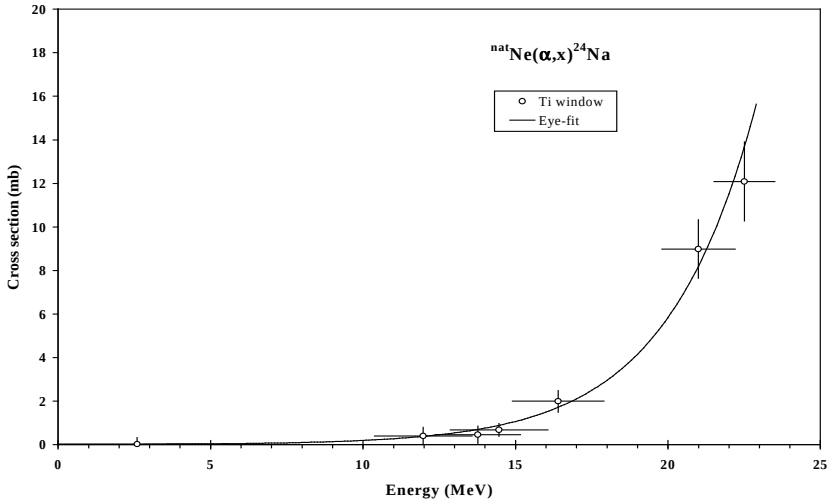

Figure 4.5. Measured excitation function of the ^{nat}Ne(α,x)^{24}Na nuclear process (from Paper 3 [86]).

$^{nat}Ne(\alpha,x)^{22}Na$ and $^{nat}Ne(\alpha,x)^{24}Na$

The excitation functions of the $^{nat}Ne(\alpha,x)^{22}Na$ and $^{nat}Ne(\alpha,x)^{24}Na$ processes are given in Figure 4.4 and Figure 4.5. The cross sections obtained by us are presented in Table 4-3 for both processes. No other data was found in the literature. Only a few data points could be measured for the formation of both ^{22}Na and ^{24}Na since the contributing processes have high thresholds. The production of ^{22}Na starts around 15 MeV and the contributing processes are the (α,pxn) and (α,xn) reactions on neon isotopes. In the case of ^{24}Na, the $^{22}Ne(\alpha,pn)$ reaction is the main contributing process, starting at about 15 MeV. The contribution of the $^{21}Ne(\alpha,p)$ reaction at lower energies is very small due to the very low isotopic abundance of ^{21}Ne in natural Ne.

Table 4-3. Measured cross sections of $^{nat}Ne(\alpha,x)^{22,24}Na$ processes (from Paper 3 [86]).

	$^{nat}Ne(\alpha,x)^{22}Na$	**$^{nat}Ne(\alpha,x)^{24}Na$**
Energy (MeV)	**σ (mb)**	**σ (mb)**
2.6 (-2.6 +3.0)		0.03 (-0.0,+0.3)
12.0 ± 1.6	4.7 ± 4.7	0.4 ± 0.4
13.8 ± 1.4	6.4 ± 6.4	0.5 ± 0.4
14.5 ± 1.6	1.2 ± 1.2	0.7 ± 0.3
16.4 ± 1.5	1.2 ± 1.2	2.0 ± 0.5
21.0 ± 1.2	32.0 ± 4.8	9.0 ± 1.4
22.5 ± 1.0	70.2 ± 10.5	12.1 ± 1.8

$^{40}Ar(\alpha,p)^{43}K$

The measured cross sections are presented in Table 4-4. The excitation function is shown in Figure 4.6. The excitation function exhibits a maximum cross section of about 70 mb at around 17 MeV. The few cross section values found in the literature and measured by Tanaka *et al.* [80] are also shown in Figure 4.6. The two results are in acceptable agreement, although the data of Tanaka *et al.* [80] seem to be shifted towards a slightly higher energy.

Table 4-4. Cross sections for the $^{40}Ar(\alpha,p)^{43}K$ reaction (from Paper 2 [89]).

Energy (MeV)	σ (mb)	Energy (MeV)	σ (mb)
8.9 ± 1.0	6.2 ± 0.8	14.6 ± 0.4	57.3 ± 6.9
9.8 ± 0.9	3.1 ± 0.4	15.2 ± 0.4	64.7 ± 7.8
10.8 ± 1.0	12.5 ± 1.5	16.0 ± 0.6	56.6 ± 6..8
10.9 ± 0.7	22.0 ± 2.7	16.2 ± 0.3	69.7 ± 8.4
11.7 ± 0.7	22.8 ± 2.8	16.7 ± 0.3	79.9 ± 9.6
12.7 ± 0.7	23.2 ± 2.8	17.5 ± 0.6	58.4 ± 7.0
12.8 ± 0.6	39.4 ± 4.8	20.1 ± 0.3	62.6 ± 7.5
13.5 ± 0.5	41.9 ± 5.1	21.4 ± 0.3	49.8 ± 6.0

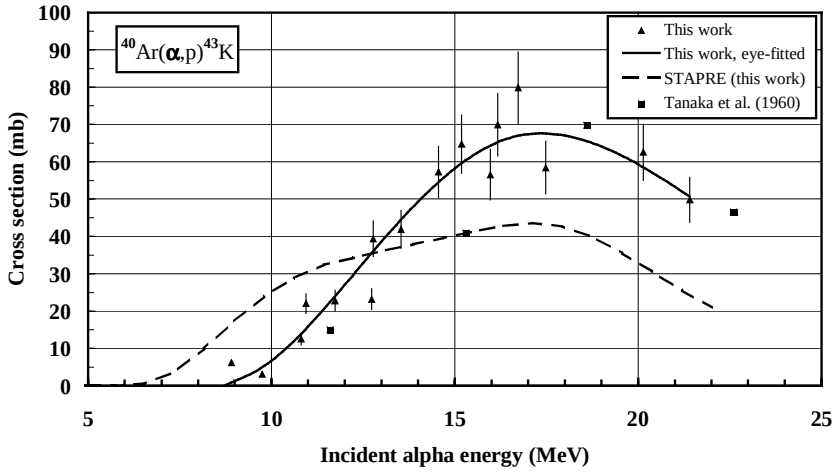

Figure 4.6. Measured excitation function of the $^{40}Ar(\alpha,p)^{43}K$ nuclear reaction (from Papers 1and 2 [88, 89]).

The experimental results were compared with results calculated with the model code STAPRE [102] which uses the Hauser-Feschbach formula for the equilibrium and the exciton model for the pre-equilibrium contribution. Neutron, proton and α-emission was taken into account and the transmission coefficients for the particles were calculated by the optical model code SCAT-2 [103]. More details of the calculation can be found in Paper 2 [89].

The calculated excitation function is shown in Figure 4.6. Comparison with the experimental data shows that above 12 MeV the calculation underestimates the experimental data while a significant overestimation is observed near the threshold. This discrepancy may indicate an inaccurate energy scale of the experimental results and/or an unsatisfactory global optical model parameter set used in the calculation. The difficulties of finding the best parameter set are well known from the nuclear physics literature. The many theoretical and experimental efforts have not yielded a global optical potential which really satisfactorily describes the alpha - nucleus interaction (Hodgson [9]). Good energy-dependent potentials have been obtained only for some particular nuclei (Avrigeanu *et al.* [10], Delbar *et al.* [104]) but unfortunately not for ^{43}K. Taking into account these problems, the agreement between the measured and calculated excitation function is acceptable.

4.5 Yields

Integral yields have been calculated from the curves fitted to the cross sections measured by us. They are presented as a function of incident particle energy in Figure 4.7 for the ^{nat}Ne(^{3}He,x)^{22,24}Na, ^{nat}Ne(α,x)^{22,24}Na processes and in Figure 4.8 for the ^{40}Ar(α,p)^{43}K reaction.

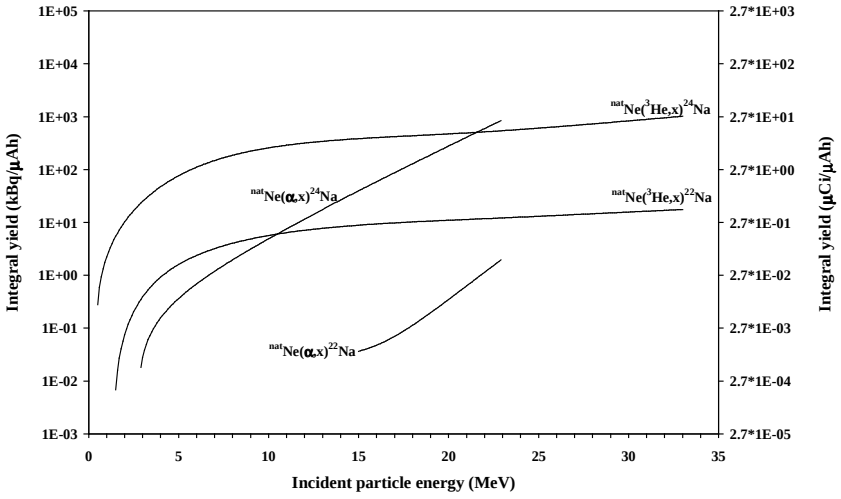

Figure 4.7. Calculated integral yields for the ^{nat}Ne(^{3}He,x)^{22,24}Na and ^{nat}Ne(α,x)^{22,24}Na processes (from Paper 3 [86]).

The yields of both ^{22}Na and ^{24}Na are higher for ^{3}He-particles than for α-particles in the investigated energy range. In the case of ^{3}He-particles, ^{22}Na and ^{24}Na are produced simultaneously in significant yields over the whole investigated energy range for ^{3}He-particles. With α-particles ^{22}Na and ^{24}Na are formed simultaneously above 12 MeV; at lower energies only ^{24}Na is produced. The ^{nat}Ne(α,x)^{24}Na process might yield significant amount of ^{24}Na above 23 MeV energy.

The amount of the ^{24}Na "contamination" in the ^{22}Na product can easily be reduced by waiting for an appropriate cooling time after EOB. This does not decrease the amount of ^{22}Na by any significant extent. For producing high purity ^{24}Na from natural neon, an alpha particle beam of less than 15 MeV is required. Obviously, use of isotopically enriched target gases would enhance the production yields and the purities.

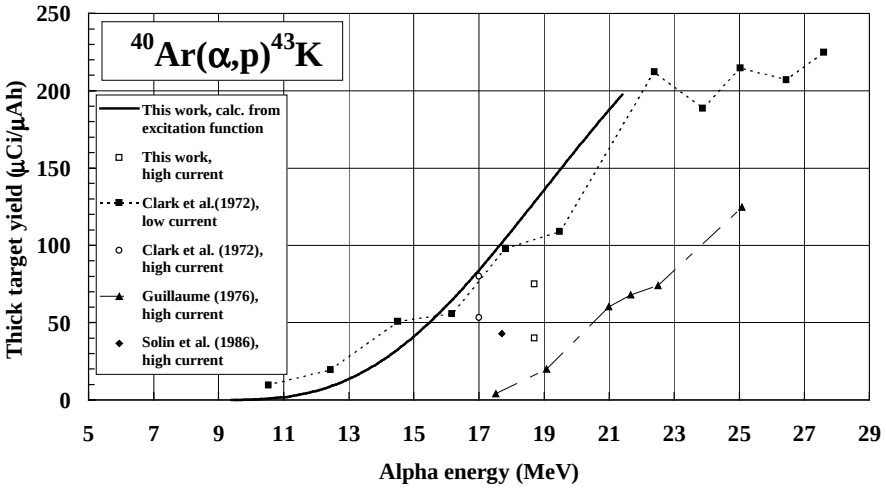

Figure 4.8. Measured and calculated thick target yields of ^{43}K produced by the ^{40}Ar(α,p)^{43}K reaction. Our data were taken from Papers 1-2 [88, 89] and from Refs. [61, 70, 72].

For the ^{40}Ar(α,p)^{43}K reaction, thick target yields measured by us and others are also shown in Figure 4.8. The integral yields calculated from the excitation function measured by us are in acceptable agreement with the experimental data of Clark *et al.* [70]. Those measurements were carried out using low beam intensities

and short irradiation times. Their 70 - 80 % recovery efficiency was taken into account by us in calculating the total activity produced. Our calculated yields in the low energy region are lower than that obtained by them. This is presumably due to their quoted large energy uncertainties in that energy region. There are large deviations between our calculated integral yields and the high current experimental thick target yields obtained by Guillaume *et al.* [61], Solin *et al.* [72] and ourselves. The production yields at high beam currents observed by us clearly indicate a significant reduction of density of target nuclei in the irradiated volume of the target gas under production circumstances.

5. Production of no-carrier added ^{24}Na and ^{43}K

This chapter describes the methods developed by us for production of no-carrier added ^{24}Na (Papers 5-6 [7, 8]) and ^{43}K (Papers 2 and 6 [89, 8]) radioisotopes at the MGC-20E cyclotron at ATOMKI.

5.1 Routes suitable for the production of ^{24}Na at the MGC-20E cyclotron

^{24}Na can be produced via different nuclear reactions. Selection of the best route needs relevant yield data. A comparison of calculated integral yields of ^{24}Na via various low energy ($E_{projectile} \leq 40$ MeV) charged particle induced routes is given in Fig. 7 in Paper 3 [86].

The ^{23}Na(d,p)^{24}Na reaction has the highest yield at each energy but the product is not carrier free. It is comparable to the ^{23}Na(n,γ)^{24}Na process. The ^{26}Mg(d,α) reaction gives also high yields even below 5 MeV but it needs isotopically enriched expensive target. The ^{nat}Mg(d,x)^{24}Na, ^{nat}Mg(p,x)^{24}Na and ^{nat}Mg(α,x)^{24}Na processes lead to significant ^{24}Na yields of no carrier added ^{24}Na at $E_{projectile} \geq 10$ MeV, 20 MeV and 30 MeV, respectively. The ^{27}Al(d,x)^{24}Na process has also a high yield above 15 MeV. The ^{27}Al(^{3}He,x)^{24}Na and ^{27}Al(p,3pn)^{24}Na processes have less significance regarding the production of ^{24}Na. In the case of ^{nat}Ne(^{3}He,x)^{24}Na process, the ^{24}Na yield increases only slightly above 10 MeV energy. The ^{nat}Ne(α,x)^{24}Na process might yield significant amount of ^{24}Na above 23 MeV energy.

At the MGC-20E cyclotron at ATOMKI, the maximum available energy of external beam of protons, deuterons, ^{3}He- and α-particles is 18 MeV, 10 MeV, 28 MeV and 20 MeV, respectively. The ^{nat}Mg(d,x), ^{nat}Ne(^{3}He,x), ^{27}Al(^{3}He,x) processes can be considered for production of no-carrier added ^{24}Na at relatively low cost at these energies.

A high intensity fast neutron irradiation facility based on the 18 MeV p(Be) source is also available at the MGC-20E cyclotron. The well known neutron induced ^{27}Al(n,α)^{24}Na reaction is also a considerable choice taking into account the spectrum, the angular distribution and the zero degree neutron yield ($1.9*10^{10}$ $n*sr^{-1}\mu C^{-1}$) of the ^{9}Be(p,n) reaction at 18 MeV [105, 106].

5.2 Production of ^{24}Na isotope via the $^{27}Al(n,\alpha)^{24}Na$ reaction

The 18 MeV p(Be) fast neutron source and the irradiation facility were designed and developed by us and they have been described in details in Paper 10 (Ref. [5]) and Refs. [3, 4, 6]. The neutron source was operated at the end of the zero degree horizontal channel of the beam-line system. The target assembly was attached to the beam pipe and to the ports of the remote controlled booster vacuum system by hinged clamps. Quick connectors were used to connect the cooling circuits and the controlling electronics in order to minimize the radiation dose to the staff persons.

A 3 mm thick beryllium disk (dia 35 mm) was used as target. The bombarded surface was cooled by a flow of 23 l/min of room temperature helium gas at p = 1.5 bar. The target assembly was separated from the vacuum by a 11 μm thick foil made of Duratherm alloy (41.5 % Co, 25.5 % Ni, 12 % Cr, 8.7 % Fe, 4 % Mo, 3.9 % W, 2 % Ti, < 1 % Mn, 0.7 % Al, < 0.03 % C; supplied by Vacuumschmelze GmbH, Hanau, Germany). The energy absorbed in the foil and in the helium gas was 170 keV at 18 MeV incident proton energy. A 30 mm long tube (internal dia 25 mm) made of aluminium embedded into a perspex insulator housing was used as secondary electron suppresser electrode in front of the target at an electric potential of - 300 V to the ground. The back side of the beryllium target was cooled by a 1 mm thick layer of water circulated by a pump in a separate closed flow circuit. The target holder was made of stainless steel and it was 3 mm thick behind the water layer. The diameter of the target spot was approximately circular and its diameter was approximately 25 mm as the spot on the window foil indicated.

The cylindrical sample holder was 25 mm in dia and it was made of perspex. The thickness of its wall was 1 mm. In the first experiment 30 g while in the second one 105 g samples of high purity Al-powder (mean particle diameter 50 μm) were irradiated. The ^{24}Na was chemically separated by a method developed by Z. Kovács [7] irradiation the powder was stirred in 800 ml boiling distilled water for 1 h. After filtration, the solution was concentrated by vacuum distillation. The average separation yield of ^{24}Na in water was 80 %. In further experiments, Al-powder was changed for 76 g of high purity of Al_2O_3 powder (mean particle diameter 30 μm) to eliminate any precipitate production and to make time consuming filtration unnecessary and increasing the average separation yield to 90 %. The idea of using Al_2O_3 powder as target material and the way of separation via simply washing the ^{24}Na out from the Al_2O_3 powder using distilled water was suggested by P. Mikecz (see Paper 6 [8]).

5.3 Production of ^{43}K isotope via the ^{40}Ar(α,p)^{43}K reaction

For the routine production of ^{43}K, at ATOMKI, some parts and design principles of a high-pressure deuterium gas target used by Schraube for neutron production via the D(d,n) reaction [107] were adapted and employed in the construction of our target chamber. A gas flow circuit shown in Figure 5.1 which is similar to the one used by Clark *et al.* [70] , was also built.

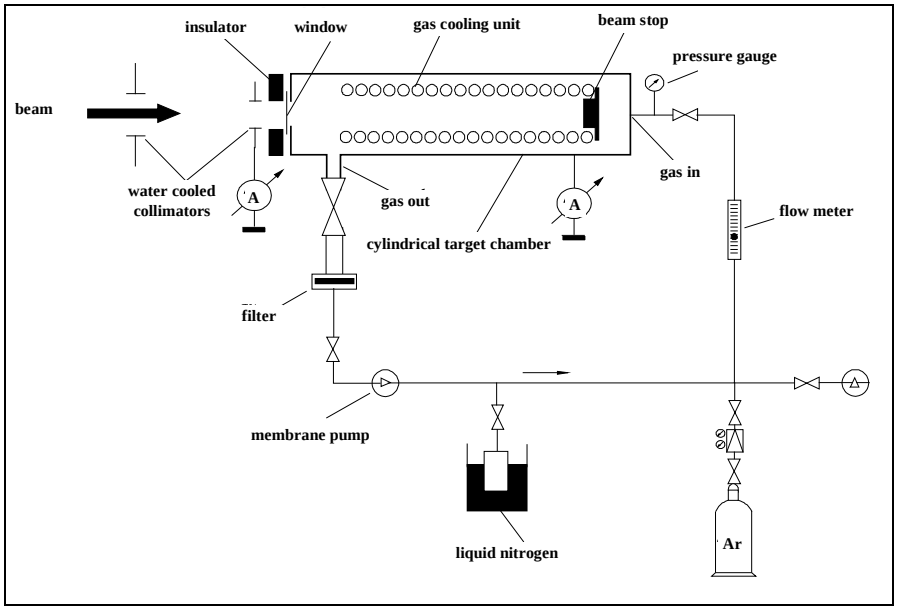

Figure 5.1. Flow target system for production of ^{43}K (from Paper 2 [89]).

The target chamber was a nickel plated brass cylinder, 32 cm in length and 9 cm in dia, equipped with a 27 cm long and 5.2 cm dia internal cooling unit (made from 8 mm dia copper tube), a water cooled beamstop, a 16 mm dia precollimator, a 12 mm dia entrance collimator and a 11 μm thick Duratherm, entrance window. The target chamber was mounted on the same horizontal beam-line mentioned above in the case of ^{24}Na production.

The target was connected, via a valve at the outlet, to an easily-removable filter holder. The outlet was located at the front side of the target where, in accordance to the excitation function, the major fraction of the activity was produced. The filter holder was only approximately 10 cm from the target and

contained a glass fibre filter, wetted with a 0.002 M HCl solution. The filter holder was connected to the inlet of a membrane pump. The outlet of this pump was connected to a flowmeter. The circuit also contained a pressure gauge connected to the valve at the inlet of the target chamber. After evacuating the target chamber and the gas handling system to 0.01 bar, they could be filled with argon gas at the desired pressure.

This system provided the possibility to use the target both in a static or batch mode and in a recirculating gas flow mode and thus the possibility to compare the two production methods. For the recirculating gas flow mode, the circuit design described above, the large diameter of the tubing between the target and the filter holder and the specific filter used ensured a very fast collection of the produced activity dispersed in the argon gas exiting the target chamber.

An initial filling gas pressure p = 1.2 bar was chosen for both methods. The observed flow rate of the pump was 47 l/min at the pressure during the irradiation (p = 1.3 bar, 10 μA)

In the flow mode, this pressure resulted in a significant fraction of the bombarding beam hitting the wall of the internal cooling spiral at high beam currents, as our optical investigations had shown (for more details see Paper 2 [89]), but it ensured a high circulation speed and an efficient recovery.

The target was irradiated with the available maximum energy α-particle beam (20.4 MeV) at currents up to 10 μA for several hours when either the static or the flow mode was employed. After irradiation the major fraction of the argon was transferred to a small gas balloon via cryopumping.

In the static or batch mode, the inner wall of the chamber was then rinsed three times with 100 ml of distilled water. The total recovery efficiency was about 90 %. after three consecutive rinses. In the flow mode, the filter was washed out four times with 5 ml of a 0.002 M HCl solution without adding carrier. This resulted in a recovery efficiency of more than 95 %.

The recovered activity also contained ^{42}K ($T_{1/2}$ = 12.4 h), when a 20.4 MeV bombarding energy was used. This contamination could be practically eliminated if the beam energy was kept below 17 MeV.

The irradiations in the flow mode at high flow rates resulted a somewhat lower activity than those in the static mode. However, the recovery procedure was

substantially more simple and quicker and higher specific activities were achieved. The total efficiency of recovery was measured repeatedly for the flow mode and was found to be 65-70 %. In most experiments, no significant change in the total efficiencies was observed if the chamber wall was cleaned between two production runs. In a few cases, abnormally small yields were obtained probably due to an unfavourable distribution of the beam intensity. In other cases, yields obtained were in full agreement with the values calculated with the model developed by Heseslius *et al.* [82] for the density reduction.

A homogenous beam intensity distribution was assumed and the excitation function measured by us was used for these calculations. Beam penetrations and shapes were also input information for the estimations. They were observed optically using a stacked windowed gas cell system at an initial pressure of p = 3 bar and at E_α = 20 MeV bombarding energy at beam currents of 1 μA, 3 μA and 5 μA, respectively (for additional details see Paper 2 [89]).

It is important to emphasise that the flow target system and the recovery method developed by us for the production of ^{43}K from argon gas is suitable also for producing ^{22}Na and ^{24}Na in no-carrier added form using beams of ^{3}He- or α-particles and natural neon gas as target meterial. Obviously, some optimisation of the production target would be necessary.

The methods developed by us and described in Chapter 5 enabled us to produce significant amount ^{24}Na and ^{43}K in no-carrier added form by simple and efficient ways routinely . Additionally, the radiation risk of the recovery of the produced radioisotopes, the chemical processing and the aliquotization could be kept at a relatively low level.

6. Study of the intensity of sap-flow of oak trees

6.1 Motivations of our water transport studies

The three most important forest comprising oak species in Hungary are robur (or pedunculate) oak *(Quercus robur),* sessile oak *(Quercus petraea)* and Austrian (or Turkey) oak *(Quercus cerris).* The dieback of *Quercus robur* has been known in Hungary since 1877. An increasing decay of *Quercus petraea* forests has been observed in many regions of the country since 1978. In 1993 and 1994 indications of decline of *Quercus cerris* have also been reported.

Many abiotic and biotic primary and secondary factors, which could be responsible for the decline, forest decay and dieback of oak species in Hungary, were discussed in a conference [108] held in Noszvaj (Hungary) in June of 1994. Until the mid-eighties air pollution and acidic precipitation were suspected to be the most important primary abiotic factors. Recently climatic changes induced by the global atmospheric warming-up are considered as the most important ones.

Approximately a decade ago a relationship had been found between air pollution and water stress of trees [109]. Water stress can also be a consequence of unusually long dry periods and many other factors. Despite of efforts, many details of the mechanisms of the development of water stress remained unknown in the case of the three oak species. Moreover, it is not fully understood, why different oak species and their healthy and unhealthy individuals respond so differently to the same environmental changes in the same area of the same forest.

The aim of our studies was to obtain information on the water distribution and measure the intensity of sap-flow in the trunks of healthy and unhealthy oak trees of the three above species by conducting concurrent field experiments.

6.2 A radioactive tracer technique for measuring the intensity of sap-flow in trees

No-carrier added ^{24}Na and ^{43}K produced by the methods described above have been used for study the intensity of sap-flow in the trunks of healthy and unhealthy oak trees. The experimental technique used and observations have been published in Papers 5 and 9 (Refs. [7 and 110]).

A radioactive tracer technique described in Paper 5 (Ref. [7]) was developed using first ^{24}Na ($T_{1/2}$ = 14.96 h) and later ^{43}K ($T_{1/2}$ = 22.3 h) radioisotopes. The half lives of these isotopes and the needed activity (20-50 MBq) make possible repeated experiments on the same tree within 5-10 days. The radiation hazard could be kept at a very low level even if the whole activity needed would pollute the soil of the test field around the investigated tree. No one has used before these radioisotopes for tracing the sap-flow of mature trees, as far as we know.

Typically 3-5 ml distilled water containing ~ 20 MBq activity of $^{24}Na^{+}$ or $^{43}K^{+}$ was injected into the xylem of healthy and unhealthy trees. A new method was developed to ensure an air bubble free injection in order to avoid the blocking and failure of the tracheas by an accidental air embolia. A second inlet port was fabricated and fit to an ordinary angiographic needle. That was used for filling the needle up with water expeling the air before knocking the needle into the trunk of the tree. The end of the needle was perforated. The injector developed by us was a special syringe like a hydraulic cylinder and it was free from any backflow. It was connected to the original inlet port of the needle to inject the active solution into the xylem.

The gamma irradiation of ^{24}Na and ^{43}K moving in the tree were detected by a four channel system containing scintillation counters fitted onto the trunk at different heights. Data were recorded by a minicomputer. The measured counts were corrected for background and decay.

6.3 Other experimental techniques used for plant-water relation studies

The intensity of water transport of healthy and unhealthy trees of different tree species was studied at different forest areas in collaboration with other groups (see the lists of authors of Refs. [7, 110, 111, 112]). Sap-flow was measured using our radioactive tracer technique and two thermometry methods (the **h**eat **p**ulse **v**elocity (HPV) technique and the Granier-method [1] (GRN) improved by us). Simultaneously water potential, leaf conductance, transpiration and **u**ltrasound **a**coustic **e**mission (UAE) were also measured in complex field experiments. Attempts were made to assess the distribution of water in trunks of different healthy and unhealthy oak trees using X-ray tomography and magnetic resonance imaging (MRI).

6.4 Results of plant-water relation studies

The results of the plant-water relation studies have been published in details in Papers 5, 7, 8 and 9 (Refs. [7, 111, 112, 110]) and in Ref. [113]. A summary of them is given below.

Forced by the gradient of water potential, sap containing the injected radioactive ions moved through interconnected conduits of xylem consisting of the porous parenchima and bundles of tracheas of different diameters having different hydraulic conductances. The water potential gradient was supposed to be a smooth continuous function of time at any point in the xylem. The response for an instantaneous injection of radioactivity into the xylem was expected to be a slow and smooth change of the counting rate lasting for hours at any point of detection.

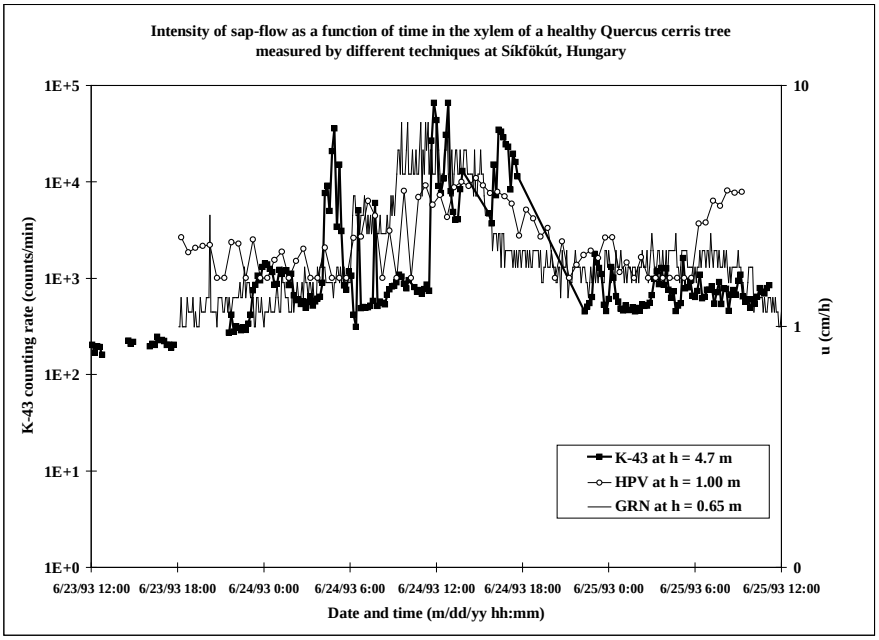

Figure 6.1. Comparison of the radiotracer technique using ^{43}K with the **H**eat **P**ulse **V**elocity (HPV) method and the Granier-method (GRN) on a healthy *Quercus cerris* tree.

Such a behaviour was observed, however, only in the case of healthy trees (Paper 5 [7]) which were well watered before the injection. In other cases, the response as a function of time was not smooth at all (see for example Figure 6.1). The sap-flow was very changeable although the usual diurnal trend could be observed in the most cases. Temporary or even pulse like increasing of the sap-flow was detected frequently. This behaviour was found in the case of both unhealthy and healthy trees of all investigated species. However, the intensity of sap-flow was very low and no pulse like behaviour was observed in the case of dying trees. The same were observed by the two thermometry methods mentioned above (Paper 9 [110]).

Concurrent thermometry measurements were also done at different positions in the trunk on the same level above the ground. They showed that the intensity of sap-flow was not homogeneous in the xylem of both healthy and unhealthy trees of all species investigated (Paper 8 [112] and Paper 9 [110]).

6.5 A qualitative model for the set up of water stress in oak trees

A qualitative phenomenological model has been developed by us to explain the above observations. In our hypothesis more conduits of xylem have high conductance in healthy trees than in unhealthy trees. Conductance of the vessels of healthy trees can dynamically changes in some range and this change is reversible in the most cases. Most of the vessels in dying trees have very low conductance and it has been altered irreversibly. The reason of the change of conductance can be understood on the basis of the mechanism described below.

The intense evaporation on the surface of leaves could induce such an intense suction that could result in a spontaneously created discontinuity in the vessels of the xylem. This is called as spontaneous or transpiration induced embolism or cavitation and it can be detected by ultrasound detectors [112, 113]. Later the cavitated trachea can be filled up with water again but only in the presence of unbound water available around the cavity The hydraulic resistance of the recovered vessel obviously decreases and thus an increased sap-flow can be observed as long as the amount of the available water and the suction are balanced.

The source of water might be the phloem [114], the xylem itself or the hardwood. The distribution of water in the xylem and in the heartwood has been investigated in healthy and unhealthy trees of *Quercus cerris* and *Quercus petraea* by Béres *et al.* by MRI [115] and computer tomography by Raschi *et al.* [113]. MRI

studies suggest that xylem and heartwood are important pools of free and weakly bound water. The molecular biological details of the triggering and the mechanism of water movement towards the cavity are unknown at present.

If no free water is available in the vicinity of the vessel then no pulses are generated and the vessel could be blocked off [7], e.g. by tylose formation permanently within some hours. This may be the situation in unhealthy oak trees affected by water stress in accordance with the observations in Ref. [116]. If the water potential gradient and/or the resistance between the cavity and the neighbourhood is low, no pulses would be generated. Probably that is the reason for the observed small number of pulses in the case of healthy *Quercus cerris* trees. Pulses are more frequent in *Quercus petraea* trees probably because the water content of the xylem is generally lower than in the case of *Quercus cerris* trees as tomograms suggest (see Paper 7 (Ref. [111]) and Refs. [113, 115]). As the number of failured vessels is increasing so the longitudinal hydraulic resistance of the pathways is also increasing and therefore the same longitudinal gradient of water potential can induce only a lower sap-flow velocity and a lower sap-volume.

The above model gives a possible explanation why dramatic upset of water stress was observed in some cases of *Quercus petraea* trees and why it caused even the sudden death of the tree in some cases.

The balance between the water uptake, storage and water loss is determined by many abiotic and biotic factors: the amount of available water and nutrients in the soil, the status of mycorrhiza-root system responsible for the water uptake, the status of the transport system of the tree, the water storage capacity, the status of stomas on the leaves and their regulation responsible for the loss of water, etc.. Water stress could set up if any of them is affected by some environmental change (e.g. increase of pH in the soil, gradation of parasites damaging any part of the system, climate changes, increased background of scattered UV light damaging leaves and stomas, etc.).

As a conclusion the above model emphasises the importance of sap-flow measurements in the identification of water stress even at an early stadium.

7. Summary

^{22}Na ($T_{1/2}$ = 2.60 y), ^{24}Na ($T_{1/2}$ = 14.96 h) and ^{43}K ($T_{1/2}$ = 22.3 h) isotopes are frequently used as tracers in various types of studies. ^{22}Na and ^{24}Na are widely used for calibration of nuclear measurement devices. The potential applications induced an investigation to find possible routes of production of no-carrier added ^{22}Na, ^{24}Na and ^{43}K at medium sized multiparticle accelerators ($E_p \leq 40$ MeV) and especially at the MGC-20E cyclotron of ATOMKI.

These studies resulted new excitation functions for the ^{nat}Ne(^{3}He,x)^{22}Na and the ^{nat}Ne(α,x)^{22,24}Na processes and for the ^{22}Ne(^{3}He,p)^{24}Na reaction from their respective thresholds up to 36 MeV in the case of ^{3}He-particles and up to 27 MeV for α-particles. New cross sections were obtained for the ^{20}Ne(d,α)^{18}F reaction in the energy range 2.8 MeV $\leq E_d \leq$ 4.3 MeV and for the ^{nat}Ne(d,x)^{18}F process in the energy range 2.8 MeV $\leq E_d \leq$ 8.5 MeV. New cross sections were measured for the ^{40}Ar(α,p)^{43}K nuclear reaction in the energy range 8.9 MeV $\leq E_\alpha \leq$ 21.4 MeV. The activation technique and stacked gas cell targets were used in these investigations.

The data obtained are new information for nuclear data evaluators and they can be used for checking, validation and/or for improvement of predictive capabilities of nuclear reaction model codes, too. They can be important for nuclear astrophysics dealing with the explosive stellar nucleosynthesis in supernova explosion. They are useful information for optimisation of radionuclide production at low energy multiparticle cyclotrons for practical applications.

Integral yields have been calculated from the curves fitted to the cross sections measured for ^{22}Na and ^{24}Na production via the ^{nat}Ne(^{3}He,x)^{22,24}Na and the ^{nat}Ne(α,x)^{22,24}Na processes and for the production of ^{43}K via the ^{40}Ar(α,p)^{43}K nuclear reaction. The excitation function of the ^{40}Ar(α,p)^{43}K reaction was calculated using the nuclear reaction model code STAPRE. The Hauser-Feschbach formula for the equilibrium and the exciton model for the pre-equilibrium contribution were used. Neutron, proton and α-emission was taken into account and the transmission coefficients for the particles were calculated by the optical model code SCAT-2. The agreement between the calculated and the measured excitation functions was acceptable. Thick target yields of ^{43}K were

calculated from the experimental data and they were compared with results published in the literature.

It has been concluded that the $^{nat}Mg(d,x)$, $^{nat}Ne(^{3}He,x)$, $^{27}Al(^{3}He,x)$ processes can be considered for production of no-carrier added ^{24}Na at the particle energies available at the MGC-20E cyclotron of ATOMKI (Debrecen, Hungary). The amount of ^{22}Na contamination can be reduced by appropriate selection of bombarding energy.

Significant amount of no-carrier added ^{24}Na was produced via the $^{27}Al(n,\alpha)$ nuclear reaction using the 18 MeV p(Be) intense fast neutron irradiation facility developed by us. A target system working in static (batch) mode or in recirculating gas flow mode has been developed to produce no-carrier added ^{43}K via the $^{40}Ar(\alpha,p)^{43}K$ nuclear reaction. The static mode and the circulated mode were compared and the observed high current yields was explained.

A new radioactive tracer technique was developed to study the intensity of water transport of healthy and unhealthy sessile oak *(Quercus petraea)* and Austrian (or Turkey) oak *(Quercus cerris)* trees. A device was constructed to inject ^{24}Na or ^{43}K into the xylem of the trunk. It enabled the injection to be free of air bubbles to avoid accidental embolism of conduits. The radioactive tracer technique was combined with a thermometry method invented by A. Granier for sap-flow measurements.

Pulse like increases of sap velocity were observed in many cases both in healthy and unhealthy *Quercus petraea* and *Quercus cerris* trees. This behaviour of sap velocity has been interpreted as an indication of the dynamic (transpiration induced) water stress of trees. It can be concluded that sap-flow measurements give the possibility of an early detection of water stress of oak trees.

8. References

[1] Granier, A.: Mesure du flux de sève brute dans le tronc du Douglas par une nouvelle méthode thermique. *Annales des Sciences des Forestières* **44 (1)**, 1 (1987).

[2] Browne, E. and Firestone, R. B.: *Tables of Radioactive Isotopes* (Ed., Shirley, V. S.), Wiley, New York (1986).

[3] Fenyvesi, A., Gál, I., Mahunka, I., Molnár, T., Tárkányi, F., Csejtei, A.: Nagy intenzitású ciklotron neutronforrások (High intensity cyclotron neutron sources). *Magyar Radiologia* **63**, 166 (1989) (in Hungarian).

[4] Molnár, T., Fenyvesi, A., Mahunka, I., Csejtei, A.: Dozimetriai mérések nagyintenzitású ciklotron neutron-forrásokon (Dosimetric measurements at high intensity cyclotron neutron sources)
Magyar Radiológia **63,** l59 (l989) (in Hungarian).

[5] Fenyvesi, A., Mahunka, I., Molnár, T.: Status report on the fast neutron irradiation facility for radiobiological purposes at the Debrecen cyclotron. *Zeitschrift für Medizinische Physik*, **1**, 30 (1991).

[6] Fenyvesi, A.: Az MGC-20 ciklotronra alapozott gyorsneutron források és alkalmazásaik. (Fast neutron sources based on the MGC-20E cyclotron and their applications)., dr. univ. Thesis, Lajos Kossuth University, Debrecen, Hungary, 1990.

[7] Béres, Cs., Fenyvesi, A., Jakucs, P., Mahunka, I., Kovács, Z., Molnár, T., Szabó, L., Ditrói, F.: Application of an MGC-20 cyclotron and methods of radioecology in solution of problems of forestry and the wood industry. *Nuclear Instruments and Methods in Physics Research B* **43,** 101 (1989).

[8] Fenyvesi, A., Mahunka, I., Tárkányi, F., Molnár, T., Béres, Cs., Kovács, Z., Mikecz, P., Szűcs, Z.
Production of ^{43}K and ^{24}Na radioisotopes in carrier-free form for use in radioecological studies at the forest area of the Síkfökút Project
in Responses of Forest Ecosystems to Environmental Changes. Eds.: Teller, A., Mathy, P., Jeffers, J.N.R., Elsevier Applied Science, London and New York, 1992, pp. 608-609.

[9] Hodgson, P. E.: Alpha particle reactions. Oxford Report OUNP-94-09 (1994).

[10] Avrigeanu, V., Hodgson, P. E. and Avrigeanu, M.: Global optical potentials for emitted alpha-particles. *Physical Review* **C49**, 2136 (1994)

[11] Janka, H-T. and Müller, E.: The first second of a Type II. Supernova: convection, accretion and shock propagation. *Astrophysical Journal* 448:L109-L113 (1995)

[12] Iben, I. Jr.: Planetary nebulae and their central stars - origin and evolution. *Physics Reports* **250**, pp. 1-94 (1995).

[13] Smith, M. S., Cecil, F. E., Firestone, R. B., Hale, G. M., Larson, D. C., Resler, D. A.: U.S. Nuclear Data Resources for a Coordinated U.S. Effort in Nuclear Data for Nuclear Astrophysics.
This is available online at:
http://www.dne.bnl.gov/~burrows/usnrdn/astrodata.html#005 (Translated into HTML by Thomas W. Burrows, Tue Feb 27 14:55 EST 1996;
Updated Fri Jun 14, 15:15 EDT 1996).

[14] Takács, S., Tárkányi, F. and Qaim, S. M.: Excitation function of ^{22}Ne(p,n)^{22}Na reaction: possibility of production of ^{22}Na at a small cyclotron. *Applied Radiation and Isotopes* **46**, 303 (1996).

[15] Gelehrter, T.D., Shreve, P.D., Dilworth, V.M.: Insulin regulation of Na/K pump activity in rat hepatoma cells. *Diabetes-USA* **33(5)** pp. 428-434 (May 1984).

[16] Mills, S. L., Basmadjian, G. P. and Ice, R. D.: Radiopharmaceauticals used in myocardial imaging. *Journal of Pharmaceutical Sciences* **70**, 1 (1981).

[17] Markov, A. K., Smith, R. O., Oglethorpe, N. C., Lehan, P. H. and Hellems, H. K.: The use of coronary vasolidators in myocardial imaging with ^{43}K. *European Journal of Nuclear. Medicine* **5**, 75 (1980).

[18] Markov, A. K., Smith, R. O., Lehan, P. H., Galyean, 3RD J. R., Rodriguez, G. and Hellems, H. K.: Detection of coronary artery disease with rapid

serial rescanning with potassium-43 at rest. *American Journal of Cardiology* **43,** 778 (1979).

[19] Rouleau, J., Bernier, R., Blanchette, J., Paquet, E., Dagenais, G. R.: Myocardial colour scan with ^{43}K in ischemic heart disease. *Journal of Canadian Association of Radiology* **28,** 262 (1977).

[20] Casella, V. R., Grant, P. M. and Igard, A. E.: The quantitative recovery and purification of spallogenic ^{43}K for nuclear medicine: a radiochemical procedure for V targets bombarded with medium-energy protons. *Journal of Radioanaytical Chemistry* **36**, 337 (1977).

[21] Skrabal, F., Glass, H. I., Clark, J. C., Jeyasingh, K. and Joplin, G. F.: A simplified method for simultaneous electrolyte studies in man utilizing ^{43}K. *International Journal of Applied Radiation and Isotopes* **20**, 677 (1969).

[22] Skrabal, F., Arnot, R. N., Helus, F., Glass, H. I., Joplin, G. F.: A method for simultaneous electrolyte investigations in man using ^{77}Br, ^{43}K, ^{24}Na. *International Journal of Applied Radiation and Isotopes* **21**, 183 (1970).

[23] Skrabal, F., Arnot, R. N., Joplin, G. F., Fraser, T. R.: The effect of glucocorticoid withdrawal on body water and electrolytes in hypopitnitary patient with adrenocortical insufficiency as investigated with ^{77}Br, ^{43}K, ^{24}Na and $^{3}H_2O$. *Clinical Sciences* **43**, 79 (1972).

[24] Johnson, J. E., Hartsuck, J. M., Zollinger, R. M. and Moore, F. D.: Radiopotassium equilibrium in total body potassium: studies using ^{43}K and ^{42}K. *Metabolism* **18**, 663 (1969).

[25] Johnson, JR R. F. and Rollo, F. D.: An evaluation of ^{81Rb} and ^{43}K for imaging using the performance index technique. *Physics in Medicine and Biology* **23**, 761 (1978).

[26] Burke, B. J. and Staddon, G. E.: The precision of a modern method for body compartment measurements using multiple isotopes. *Clinical Chemica Acta* **117**, 85 (1981).

[27] Khan, R. A.: Isotopically labelled compounds in the study of extracellular fluid space in dog bone. *Med. Biol.* **57**, 107 (1979)

[28] Isomaa, B., Hägerstrand, H., Paatero, G. and Engblom, A. C.: Permeability alterations and antihaemolysis induced by amphiphiles in human erithrocytes. *Biochem. Biophys. Acta* **860**, 510-524 (1986).

[29] Albert, P. Blondiaux, G., Debrun, J. L., Giovagnoli, A. and Valladon, M.: Thick target yields for the production of radioisotopes. In *Handbook of Activation Cross Sections, Technical Report Series No. 273*, p. 537, International Atomic Energy Agency, Vienna, Austria (1987).

[30] Iljonov, A. S., Semenov, V. G., Semenova, M. P., Sobolevsky, N. M. and Udovenko, L. V.: *Radionuklidproduktion bei mittleren Energien, Landolt-Börstein, Neue Serie 13a* (Edited by Schopper, H.). Springer-Verlag, Berlin (1991).

[31] Dmitrijev, P. P.: Radionuclide yield in reactions with protons, deuterons, alpha particles and helium-3 (Handbook)., Report INDC(CCP)-263/G+CN+SZ, International Atomic Energy Agency, Vienna, Austria (1986).

[32] Reddy, G. N., Beer, H.-F. and Schubiger, P. A.: Determination of excitation functions for $^{20}Ne(p,p2n)^{18}Ne \rightarrow {}^{18}F$ and $^{20}Ne(p,2pn)^{18}F$ and a reexamination of production of $[^{18}F]F_2$ with protons on Neon. In *Proceedings of the Fifth International Workshop on Targetry and Target Chemistry, September 19-23, 1993*, Brookhaven National Laboratory, Upton, New York, North Shore University Hospital, Manhasset, New York, USA. Eds.: Dahl, J. R., Ferrieri, R., Finn, R., Schlyer, D. J., BNL-61149, Informal Report, Brookhaven National Laboratory, Upton, New York, 11973-5000 (1994).

[33] Norman, E. B., Chupp, T. E., Lesko, K. T., Grant, P. J. and Woodruff, G. L.: ^{22}Na production cross section from the $^{19}F(\alpha,n)$ reaction., *Physical Review* **C 30**, 1339 (1984).

[34] Bowen, L. H., Irvine, Jr., J. W. and Morgan, I. L.: Nuclear excitation functions and thick target yields. ^{19}F, ^{23}Na, $^{75}As(d,t)$, and ^{23}Na, $^{75}As(d,p)$. *Physical Review* **127,** 1698 (1962).

[35] Lange, J., Münzel, H. and Gantner, E.: Deuteronen-Anregungsfunktionen für die Bildung von ^{24}Na und ^{22}Na aus ^{23}Na unter Verwendung von NaCl-Kohlenstoff-Folien., *Radiochimica Acta* **11**, 121 (1969).

[36] Meadows, J. W. and Holt, R. B.: Some excitation functions for protons on Magnesium., *Physical Review* **83**, 1257 (1951).

[37] Cohen, B. L., Newman, E., Charpie, R. A. and Handley, T. H.: (p,pn) and (p,αn) excitation functions., *Physical Review* **94**, 620 (1954).

[38] Bodemann, R., Busemann, H., Gloris, M., Leya, I., Michel, R., Schiekel, T., Herpers, U., Holmqvist, B., Condé, H., Malmborg, P., Dittrich-Hannen, B. and Suter, M.: New measurements of the monitor reactions ^{27}Al(p,x)^{7}Be, ^{27}Al(p,3p3n)^{22}Na, ^{27}Al(p,3pn)^{24}Na and ^{65}Cu(p,n)^{65}Zn. *Progress report on nuclear data research in the Federal Republic of Germany for the period April 1, 1994 to March 31, 1995* (Edited by Qaim, S. M.), p. 29, NEA/NSC/DOC (95) 10, INDC-Ger-040, JÜL-3086 (1995).

[39] Michel, R., Brinkmann, G., Galas, M. and Stück, R.: Integral excitation functions of charged particle induced reactions for energies up to 45 MeV/A. *Progress Report on Nuclear Data Research in the Federal Republic of Germany for the Period April 1, 1981 to March 31, 1982* (Eds.: Cierjaks, S., and Behrens, H.), NEA-NDC(E)232U Vol. 5, p. 36, (1982).

[40] Martens, U. and Schweimer, G. W.: Production of ^{7}Be, ^{22}Na, ^{24}Na and ^{28}Mg by irradiation of ^{27}Al with 52 MeV deuterons and 104 MeV alpha particles., *Zeitschrift für Physik* **233**, 170 (1970).

[41] Cochran, D. R. F. and Knight, J. D.: Excitation functions of some reactions of 6- to 24-MeV ^{3}He ions with carbon and aluminium. *Physical Review* **128**, 1281 (1962).

[42] Brill, O. D.: ^{3}He-light nucleus interaction cross sections, *Sov. J. Nucl. Phys.* **1**, 37 (1965).

[43] Lamb, J. F.: Radioactivation by ^{3}He bombardment: A practical analytical system. (Ph. D. Thesis), Rep. UCLR-18981 (1969).

[44] Wilson, R. L., Frantsvog, D. J., Kunselman, A. R., Détraz, C., and Zaidis, C. S.: Excitation functions of reactions induced by ^{1}H and ^{2}H ions on natural Mg, Al and Si., *Physical Review* **C** 13, 976 (1976).

[45] Cohen, B. L., Reynolds, H. L. and Zucker, A.: Comparison of nitrogen and proton induced nuclear reactions, *Physical Review* **96**, 1617 (1954).

[46] Meadows, J. W. and Holt, R. B.: Excitation functions for proton reactions with Sodium and Magnesium., *Physical Review* **83**, 47 (1951).

[47] Bartell, F. O. and Softky, S.: Excitation functions for deuterons and protons on Mg., *Physical Review* **84,** 463 (1951).

[48] Rohm, H. F., Verwey, C. J., Steyn, J. and Rautenbach, W. L.: Excitation functions for the ^{24}Mg(d,α)^{22}Na, ^{26}Mg(d,α)^{24}Na and ^{27}Al(d, αp)^{24}Na reactions., *J. Inorg. Nucl. Chem.* **31,** 3345 (1969).

[49] Frantsvog, D. J., Kunselman, A. R., Wilson, R. L., Zaidis, C. S. and Détraz, C.: Reactions induced by ^{3}He and ^{4}He ions on natural Mg, Al and Si., *Physical Review* **C** 25, 770 (1982).

[50] Hintz, N. M. and Ramsey, N. E.: Excitation functions to 100 MeV., *Physical Review* **88**, 19 (1952).

[51] Cumming, J. B: Monitor reactions for high energy proton beams., *Ann. Rev. Nucl. Part. Sci.* **13**, 261 (1963).

[52] Miyano, K.: The ^{7}Be, ^{22}Na and ^{24}Na production cross sections with 22 to 52 MeV protons on ^{27}Al., *Journal of the Physical Society of Japan* **34**, 853 (1973).

[53] Holub, R., Fowler, M., Yaffe, L. and Zeller, A.: Formation of ^{24}Na in "fission-like" reactions., *Nuclear Physics* **A 228**, 291 (1977).

[54] Grütter, A.: Excitation functions for radioisotopes produced by proton bombardment of Cu and Al in the energy range of 16 to 70 MeV., *Nuclear Physics* **A 383**, 98 (1982).

[55] Schneider, A. J., Sisterson, J. M. and Koehler, A. M.: Measurement of cross sections for aluminium-26 and sodium-24 induced by protons in aluminium., *Nuclear Instruments and Methods* **B 29**, 271 (1987).

[56] Weinreich, R., Probst, H. J. and Qaim, S. M.: Production of chromium-48 for applications in life sciences. *International Journal of Applied Radiation and Isotopes* **31**, 223 (1980).

[57] Lindsay, R. H. and Carr, R. J.: He-induced reactions of Al and Mg., *Physical Review* **118**, 1293 (1960).

[58] Michel, R., Brinkmann, G. and Herr, W.: Alpha-induced production of ^{24}Na and ^{22}Na from Al., Report INDC(GER)-22/L+SPECIAL, International Atomic Energy Agency, Vienna, Austria (1980).

[59] Ruth, T. J.: The production of ^{18}F-F_2 and ^{15}O-O_2 sequentially from the same target chamber. *International Journal of Applied Radiation and Isotopes* **36**, 107 (1985).

[60] Saam, B., Skalsey, M. and Van House, J.: Measurement of the cross section ^{22}Ne(p,n)^{22}Na. *Physical Review* **40**, R1563 (1989).

[61] Guillaume, M.: Production en routine par cyclotron de fluor-18 et potassium-43 á usage médical au moyen d`une cible gazeuse télécommandée. *Nucl. Instr. Meth.* **36**, 185 (1976).

[62] Nozaki T., Iwamoto M. and Ido T.: Yield of ^{18}F for various reactions from oxygen and neon. *International Journal of Applied Radiation and Isotopes* **25**, 393 (1974).

[63] Backhausen H., Stöcklin G. and Weinreich R.: Formation of ^{18}F via its ^{18}Ne precursor: excitation functions of the reactions ^{20}Ne(d,x)^{18}Ne and ^{20}Ne(^{3}He,αn)^{18}Ne. *Radiochimica Acta* **29**, 1 (1981).

[64] Lagunas-Solar, M. C. and Carvacho, F.: Cyclotron production of PET radionuclides: No-carrier added Fluorine-18 with high-energy protons on natural neon gas targets., *Applied Radiation and Isotopes* **46**, 833 (1995).

[65] Helus, F., Uhlir, V., Gasper, H. and Maier-Borst, W.: Contribution to the cyclotron targetry, IV. Measurement of ^{18}F, ^{21}Na and ^{23}Ne production yields in deuteron induced reaction on neon gas., *Journal of Radioanalytical and Nuclear Chemistry, Articles* **198,** 247 (1995).

[66] Merchel, S.: Radiochemische Unterschungen über die (^{3}He,^{7}Be)-Reaktion an leichten Targetkernen, Diplomaarbeit, Fach Chemie an der Matematisch-Naturwissenschaftlichen Fakultät der Universität zu Köln, Köln/Jülich (1995).

[67] Merchel S. and Qaim S. M.: Excitation functions of (^{3}He,^{7}Be)-reactions on light mass target elements, *Radiochimica Acta*, in press.

[68] de Britto J. L. Q., de Sousa A. S. F. and da Silva A. G.: Thick target yield of ^{22}Na using 27 MeV α-particles on natural Ne. J. *Radioanalytical and Nuclear Chemistry Letters* **187**, 143 (1994).

[69] Dyson, N.A. and Francois, P.E.: The preparation of potassium-43 using an interrupted cyclotron beam. *Int. J. Appl. Radiat. Isot.* **7**, 150(1959).

[70] Clark, J. C., Thakur, M. L. and Watson, I. A.: The production of potassium-43 for medical use. *Int. J. Appl. Radiat. Isot.* **23**, 329 (1972).

[71] Virtanen, P. and Wilcken, H.: Production of ^{43}K using Ar-gas target. *The Accelerator at Åbo Akademi, Triennial Report, 1976-1978*, p. 51 (1979).

[72] Solin, O., Bergman, J. and Aho, K.: Production of ^{43}K. In *The Abo Akademi Accelerator Laboratory, Biennial Report, 1985-1986*, p. 70 (1987).

[73] Oka, Y., Kato, T. and Namura, K.: A study on the yield of (γ,p) reactions with 20 MeV bremsstrahlung. *Bulletin of the Chemical Society of Japan* **41**, 380 (1968).

[74] Gray, F. C., Cole, C. M., Meaburn, G. M. and Bruhhart, G.: Electron linear accelerator production of ^{43}K. *Journal of Nuclear Medicine* **14**, 931 (1973).

[75] Poggenburg, J. K.: ^{43}K: The reactor production , physical properties and potential availability of a useful radioisotope. *Journal of Nuclear Medicine* **12**, 457 (1971).

[76] O`Brien, H. A. and Hupf, H. B.: ^{43}K and ^{67}Cu for medical applications. *Journal of Nuclear Medicine* **9**, 340 (1968).

[77] Erdal B. R., Grant P. M., Casella V. R., Ogard A. E. and O'Brien H. A. (1975) Spallation cross sections and the LAMPF medical radioisotope program. In *Nuclear Cross Sections and Technology, Proceedings of the Conference on Nuclear Cross Sections and Technology, Washington D. C., 1975*, **Vol. 2**, p. 492, National Bureau and Standards Special Publication 425, October, 1975, Washington, U.S.A.

[78] O`Brien, H. A., Grant, P.M. and Ogard, A.E.: The LASL medical radioisotope research program: radiochemistry problems and new developments. *Progresses in Nuclear Medicine* **4**, 93 (1978).

[79] Qaim, S. M. and Probst, H. J.: Excitation functions of deuteron induced nuclear reactions on Vanadium with special reference to the product of ^{43}K: systematics of (d,xn) reaction cross sections relevant to the formation of highly neutron defficient radioisotopes. *Radiochimica Acta* **35**, 11 (1984).

[80] Tanaka, S., Furukawa, M., Iwata, S. Yagi, M. and Amano, H.: Reactions of argon-40 with alpha-particles. *Journal of the Physical Society of Japan* **15**, 952 (1960).

[81] Waters, S. L., Watson, I. A. and Downey, S.: The production of ^{43}K using in owned gas target. *Journal of Labelled Compounds and Radiopharmaceauticals* **23**, 1383 (1986).

[82] Heselius, S-J., Lindblom, P. and Solin, O.: Optical studies of the influence of an intensive ion beam on high-pressure gas targets. *International Journal of Applied Radiation and Isotopes* **33**, 653 (1982).

[83] Tárkányi, F., Takács, S., Heselius, S.-J., Solin, O. and Bergman, J.: Static and dynamic effects in gas targets used for medical radioisotope production., *Nuclear Instruments and Methods A*. (in print).

[84] Deconninck, G.: Introduction to radioanalytical physics. Nuclear Method Monographs 1, Akadémiai Kiadó, Budapest, 1978.

[85] Bonardi, M.: The contribution to nuclear data for biomedical radioisotope production from the Milan cyclotron laboratory. In *Proceedings of the IAEA Consultants' Meeting on Data Requirements for Medical Radioisotope Production, 20-24 April 1984, Tokyo, Japan*. Ed.: Okamoto, K., p. 98, INDC(NDS)-195/GZ, IAEA Nuclear Data Section, Wagramerstasse 5, A-1400 Vienna, Austria, January 1988.

[86] Fenyvesi, A., Merchel, S., Takács, S., Szelecsényi, F., Tárkányi, F. and Qaim, S. M.: Excitation Functions of ^{nat}Ne(^{3}He,x)^{22,24}Na and ^{nat}Ne(α,x)^{22,24}Na Processes: Investigation of Production of ^{22}Na and ^{24}Na at a Medium-Sized Cyclotron. *Radiochimica Acta*, (accepted for publication).

[87] Fenyvesi, A., Takács, S., Merchel, S., Pető, G., Szelecsényi, F., Molnár, T., Tárkányi, F. and Qaim, S. M.: Excitation Functions of Charged Particle Induced Reactions on Neon: Relevance to the Production of ^{22,24}Na and ^{18}F. Presented at the *International Conference on Nuclear Data for Science and Technology, 19-24 May, 1997, Trieste, Italy* and submitted for publication in the Proceedings of the Conference (in press).

[88] Fenyvesi, A., Tárkányi, F., Szelecsényi, F., Takács, S., Szűcs, Z., Molnár, T., Sudár, S.: Measurement of excitation function and thick target yield of the ^{40}Ar(α,p)^{43}K reaction. In *Proceedings of the International Conference on Nuclear Data for Science and Technology, Gatlinburg, Tennessee, May 9-13, 1994*, Ed.: J. K. Dickens, American Nuclear Society, Inc., 555 N. Kensington Ave., La Grange Park, Illinois 60525, USA, 1994, pp. 406-408.

[89] Fenyvesi, A., Tárkányi, F., Szelecsényi, F., Takács, S., Szűcs, Z., Molnár, T., Sudár, S.: Excitation function and thick target yield of the ^{40}Ar(α,p)^{43}K reaction: production of ^{43}K. *Applied Radiation and Isotopes* **46**, 1413 (1995).

[90] Szelecsényi, F., Tárkányi, F.: A horizontal beam-line for practical irradiations. *Atomki Annual Report 1988*, 116, (1989).

[91] Tárkányi, F., Qaim, S. M. and Stöcklin, G.: Excitation functions of ^{3}He- and α-particle induced nuclear reactions on natural krypton: production of ^{82}Sr at a compact cyclotron. *Applied Radiation and Isotopes* **39**, 135 (1988).

[92] Tárkányi, F., Qaim, S. M. and Stöcklin, G.: Excitation functions of ^{3}He-particle induced reactions on enriched ^{82}Kr and ^{83}Kr. *Radiochimica Acta* **43**, 185 (1988).

[93] Józsa, M., Máté, Z., Veress, Z. and Zolnai, L.: Calibration of the analyzing magnet of the MGC cyclotron. *ATOMKI Annual Report 1988*, 7 (1989)

[94] Kormány, Z.: A new method and apparatus for measuring the mean energy of cyclotron beams. *Nucl. Instr. Meth.* **A337**, 258 (1994).

[95] Takács, S., Sonck, M., Scholten, B., Hermanne, A. and Tárkányi, F.: Excitattion function of deuteron induced nuclear reactions on ^{nat}Ti up to 20 MeV for monitoring deuteron beams. *Applied Radiation and Isotopes* **48**, 657 (1997).

[96] Tárkányi, F., Szelecsényi, F. and Kopecký, P.: Cross section data for proton, ^{3}He- and α-article induced reactions on ^{nat}Ni, ^{nat}Cu and ^{nat}Ti for monitoring beam performance. In *Proceedings of the International Conference on Nuclear Data for Science and Technology, Jülich, Germany, May 1991* (Ed.: Qaim, S. M.), Springer-Verlag, Berlin (1992), p. 529.

[97] Williamson, C. F., Boujot, J. P. and Picard, J.: *Tables of range and stopping power of chemical elements for charged particles of energy 0.05 to 500 MeV*. Rapport CEA-R-3042, Saclay, France (1966).

[98] Ziegler, J. F.: *Handbook of Stopping Cross-Sections for Energetic Ions in all Elements*, Vol.5, Pergamon Press, Oxford (1980).

[99] Tárkányi, F., Szelecsényi, F. and Takács, S.: Determination of effective bombarding energies and fluxes using an improved stacked-foil technique. *Acta Radiol. Suppl.* **376**, 72 (1991).

[100] Piel, H., Qaim, S. M. and Stöcklin, G.: Excitation functions of (p,xn) reactions on ^{nat}Ni and highly enriched ^{62}Ni: Possibility of production of medically important radioisotope ^{62}Cu at a small cyclotron. *Radiochimica Acta* **65**, 81 (1992).

[101] Endt, P. M.: Energy levels of A = 21 - 44 nuclei (VII)., *Nucear. Physics A* **251**, 1 (1990)

[102] Uhl, M. and Strohmayer, B.: Computer code for particle induced activation cross sections and related quantities. *IRK 76/01 and the Addenda to the Report*, Institut für Radiumforschung and Kernphysik, Vienna, Austria (1976).

[103] Bersillon, O.: SCAT-2 optical model code. Report CEA-N-2227.

[104] Delbar, Th., Grégoire, G., Paic, G., Ceulener, R., Michel, F., Vanderpoorten, R., Budzanowski, A., Dixon, W. R., Storey, R. S. and Simpson, J. J.: Life times of ^{44}Ti levels. *Nuclear Physics A* **202**, 579 (1973).

[105] Lone, M. A., Bigham, C. G., Fraser, J. S., Schneider, H. R., Alexander, T. K., Ferguson, A. J. and McDonald, A. B.: *Nucl. Instr. Meth.* **143**, 331 (1977).

[106] Lone, M. A., Ferguson, A. J. and Robertson, B. C.: *Nucl. Instr. Meth.* **189**, 515 (1981).

[107] Schraube, H.: Die Erzeugung und Messung schneller Neutronen an einen Kompaktzyklotron für die Anwendung in der Strahlentherapie. *GSF-Bericht,* **S465** (1977).

[108] *Erdő és Klíma Konferencia, Noszvaj, 1994. junius 1-3, (Proceedings of Conference on Forests and Climate, Noszvaj, Hungary, June 1-3, 1994),* (Edited by Tar, K., Berki, I. and Kiss, Gy.), KLTE 94-041. Kossuth Lajos Tudományegyetem, Debrecen (in Hungarian) (1995).

[109] Woodward, F.I.: Climate and plant distribution, p. 174. Cambridge University Press, Cambridge, UK (1987).

[110] Fenyvesi, A., Béres Cs., Ridder, H.-W., Raschi, A., Molnár, T., Röfler, J., Lakatos, T. and Csiha, I.: Sap-flow velocities and distribution of wet-wood in trunks of healthy and unhealthy *Quercus robur*, *Quercus petraea* and *Quercus cerris* oak trees in Hungary. *Chemosphere* (in press).

[111] Raschi, A., Tognietti, R., Ridder, H.-W., Béres, Cs., Fenyvesi, A.: The use of computer thomography in the study of pollution effects on oak trees. *Agricoltura Mediterranea, Special Volume, Responses of Plants to Air Pollution*, 298 (1995).

[112] Tognietti, R., Rasch,i A., Béres, C., Fenyvesi, A., Ridder, H.-W.: Comparison of sap flow, cavitation and water status of *Quercus petraea* and *Quercus cerris* trees with special reference to computer tomography. *Plant, Cell and Environment* **19**, 928 (1996).

[113] Raschi, A., Tognietti, R., Ridder, H.-W. and Béres, C.: Water in the stems of sessile oak (Quercus petraea) assessed by computer tomography with concurent measurement of sap velocity and ultrasound emission. *Plant, Cell and Environment* **18**, 545 (1995).

[114] Salleo, S., Lo Gullo, M. A., De Paoli, D. and Zippo, M.: Refilling of cavitated xylem conduits in young plants of Laurus nobilis L.: A possible Mechanism. *XXth World Congress of the International Union of Forestry Research Organisations, 6-12 August 1995*, Tampere, Finnland. Abstract No.: S2.01-10 Xylem Physiology, Part 2 (http://www.metla.fi/conf/iufro95abs/d2pap25.htm)

[115] Béres, Cs., Fenyvesi, A., Raschi, A., Ridder, H.-W.: Field experiment on water transport of oak trees studying by computer tomograph and magnetic resonance imaging. *Chemosphere* (in press) (1997).

[116] Jakucs, P. and Tóth, J. A.: Blocking off of tracheas in the xylem of sickened sessile oak (*(Quercus petraea)* trees, Az Erdő **28**, 358-365, (in Hungarian) (1988).

Acknowledgements

At this point, I want to acknowledge my advisor and present supervisor Dr. Ferenc Tárkányi, C.Sc., head of the Cyclotron Application Department of the Institute of Nuclear Research of the Hungarian Academy of Sciences (ATOMKI, Debrecen, Hungary) for his guidance. His active support has been the utmost importance for the progress of my work. I also thank him for his many helpful suggestions about the presentation of the material.

I am greatly indebted to my former supervisor Dr. Imre Mahunka, C.Sc., who directed my steps in the development of the fast neutron irradiation facility and in the application of the radioisotope tracer technique for measuring the sap-flow of trees.

My very special gratitude to assistant lecturer Csilla Béres, dr. univ., Institute of Ecology, Kossuth University, Debrecen. She inspired, organized and instructed numerous remarkable field experiments and workshops to enable us studying the different aspects of the water transport of oak trees in fruitful international collaborations.

I also want to express my gratitude to my other co-authors, Prof. Dr. Pál Jakucs, Prof. Dr. Syed M. Qaim, Imre Csiha, Ph.D., András Csejtei, med. univ. dr., Ferenc Ditrói, Ph.D., István Gál, Zoltán Kovács, C.Sc., Tamás Lakatos, PhD student, Ms. Sielke Merchel, Pál Mikecz, dr. univ., Tamás Molnár, dr. univ., Gábor Pető, C.Sc., Antonoio Raschi, Ph.D., Hans-Werner Ridder, Dipl.-Phys., János Röfler, PhD student, Sándor Takács, dr. univ., Roberto Tognietti, Ph.D., Sándor Sudár, C.Sc., Zoltán Szűcs, dr. univ., assistant lecturer László Szabó, dr. univ. and Ferenc Szelecsényi, dr. univ.. Their contribution to various parts of our joint studies have been crucial for the progress of this work.

I am very grateful to all the former and present colleagues including the directorates of ATOMKI and the Institute of Ecology, Kossuth University, Debrecen who, in one way or another have given their support during the performance of this work.

Part of measurements of the excitation functions of the $^{nat}Ne(^{3}He, x)^{22,24}Na$ and $^{nat}Ne(\alpha, x)^{22,24}Na$ processes was carried out in the frame of the bilateral agreement administered by the Intergovernmental Committee of the German-

Hungarian Co-operation in Science and Technology (Project No. 13/X 231.7 in Germany and Project No. D/119 in Hungary). The financial support was provided by the Ministry of Education, Research and Technology (BMBF, Bonn) and the Government Office for Technical Development (Budapest). Much of the sap-flow measurements was done in the framework of different projects supported by the National Science Foundation of Hungary (OTKA). Contract Numbers are F 5068, 1711 and T006227. Complex plant-water relation studies were supported in part by the Supervisory of Gambling of Hungary and by a project of the European Community (EV5V-CT92-0093). These supports are gratefully acknowledged.

Finally I wish to express my warmest thanks to my wife Edith and our children Edith and Boglárka and my mother and my late father for their patience and support throughout the years.

Magyar nyelvű összefoglaló

Deuteron, ^{3}He- és α-részecskék által ^{nat}Ne és Ar céltárgyakban kiváltott néhány magreakció gerjesztési függvénye:

^{22,24}Na és ^{43}K radioizotópok termelése és alkalmazása tölgyfák nedváramlásának nyomjelzésére

doktori (PhD) értekezés tézisei

dr. univ. Fenyvesi András

Kossuth Lajos Tudományegyetem
Debrecen, 1997

1. Előzmények

1987 -ben a Kossuth Lajos Tudományegyetem (KLTE) Ökológia Tanszékének és az MTA Atommagkutató Intézete (ATOMKI, Debrecen) Ciklotron Alkalmazási Osztályának munkatársai egy olyan radioizotóp nyomjelzéses módszer kifejlesztését tűzték ki célul, mely alkalmas fák vízáramlásának terepi körülmények között történő tanulmányozására. A vízárammal szállítódó egyértékű pozitív ionok valamely radioizotópjának "no-carrier added" formában történő előállítása látszott legcélszerűbnek. A tervezett vizsgálatok színhelyén, a KLTE Síkfőkút Project kísérleti erdőterületén betartandó hatóságilag előírt sugárvédelmi szabályok alapján a rövid felezési idejű ^{24}Na ($T_{1/2}$ = 14.96 h), ^{42}K ($T_{1/2}$ = 12.36 h) és a ^{43}K ($T_{1/2}$ = 22.3 h) radioizotópok jöhettek elsősorban számításba. Ezeket az izotópokat sokféle nyomjelzéses módszerben alkalmazák már. Hosszú ideig tartó nyomjelzés esetén a ^{22}Na ($T_{1/2}$ = 2.6 y) használata a célszerűbb. A ^{22}Na és ^{24}Na izotópokat gyakran használják nukleáris mérőberendezések hitelesítésére is. A potenciális alkalmazási lehetőségek arra késztettek bennünket, hogy megvizsgáljuk ezen izotópok előállításának lehetőségeit közepes energiájú ($E_p \leq 40$ MeV) gyorsítók, különösen pedig az ATOMKI MGC-20E ciklotronja mellett.

Korábban már kifejlesztettük az MGC-20E ciklotronra alapozott 18 MeV p(Be) nagyintenzitású gyorsneutron forrást ezért a ^{27}Al(n,α)^{24}Na reakció útján történő termelés volt a legegyszerűbben és leggyorsabban kivitelezhető. Alumínium, később Al_2O_3 port aktiváltunk fel gyorsneutronokkal és kémiai úton nyertük ki a ^{24}Na -ot. Az elválasztás kényelmetlenségei valamint a töltöttrészecske nyalábok esetén megvalósítható nagyobb részecske fluxusok arra sarkalltak bennünket, hogy az említett radioizotópok "no-carrier added" formában történő előállítására alkalmas egyéb reakciókat is megvizsgáljuk.

Az irodalom áttekintése során kiderült, hogy a proton, deuteron, ^{3}He- és α-részecskék által neon izotópokon kiváltott magreakciók gerjesztési függvényeire vonatkozó adatok még 20 MeV alatt is alig ismertek. Hasonló eredményre jutottunk a ^{40}Ar(α,p)^{43}K esetében is noha ez az egyetlen olyan reakció, amely kis gyorsítók mellet is használható ^{43}K termelésre. A gerjesztési függvényekere vonatkozó elméleti számolásokat sem találtunk ez utóbbi reakcióra, noha az (α,p) reakciók mechnizmusát leíró modellek validálásához minél több adatra volna szükség.

Az asztrofizikai számítások szerint a nagy tömegű, szilíciumot is égető magányos csillagok neonban gazdag tartományaiban a hőmérséklet elérheti akár a $4*10^9$ K -t is. Az ilyen csillagok szupernova robbanása során keletkező lökéshullámban egyes számítások szerint $T > 4.5*10^9$ K hőmérséklet adódik. A Q-értékek valamint a Coulomb-gátak magassága alapján a $^{22}Ne(p,n)^{22}Na$, $^{20}Ne(d,\alpha)^{18}F$, $^{20}Ne(^3He,p)^{22}Na$ és a $^{20}Ne(^3He,n)^{22}Mg \rightarrow ^{22}Na$ reakciókra vonatkozó adatok esetleg a nukleáris asztrofizikai adatbázisok és szupernova modell kódok számára is hasznosak lehetnek.

Megállapítható, hogy a proton, deuteron, ^{3}He- és α-részecskék által neon izotópokon kiváltott magreakciók valamint a $^{40}Ar(\alpha,p)^{43}K$ reakció gerjesztési függvényére vonatkozó adatok mind a magfizika, mind az asztrofizika továbbá az alacsony energiájú gyorsítókkal történő radioizotóp termelés optimalizálása szempontjából értékesek lehetnek.

2. Gerjesztési függvények mérése során kapott új tudományos eredmények

A fentiek ismeretében megmértük néhány reakció gerjesztési függvényét aktivációs módszerrel. A kísérletek során gázcéltárgyakat használtunk. A besugárzások, a gamma spektrumok mérése és kiértékelése az MTA ATOMKI valamint az Institut für Nuklearchemie, Forschungszentrum Jülich GmbH (Jülich, Németország) kísérleti bázisának felhasználásával nemzetközi együttműködés keretében történtek.

Meghatározó szerepem volt az alábbi új tudományos eredmények elérésében:

1. A $^{nat}Ne(d,x)^{18}F$ folyamat esetében 7 új hatáskeresztmetszet adódott a 2.8 MeV $\leq E_d \leq$ 8.5 MeV energia tartományban, melyek közül 2 pont tisztán a $^{20}Ne(d,\alpha)^{18}F$ reakcióra vonatkozik a 2.8 MeV $\leq E_d \leq$ 4.3 MeV tartományban.

2. Elsőként mértük a $^{nat}Ne(^3He,x)^{22}Na$ folyamat hatáskeresztmetszetét és 35 új pontot kaptunk a 1.5 MeV $\leq E_{3He} \leq$ 33.3 MeV tartományban.

3. Elsőként mértük a $^{nat}Ne(^3He,x)^{24}Na$ folyamat hatáskeresztmetszetét, melynek során 23 új pont adódott a 1.5 MeV $\leq E_{3He} \leq$ 33.3 MeV tartományban, és ezek mindegyike tisztán a $^{22}Ne(^3He,p)^{24}Na$ reakcióra vonatkozik.

4. Elsőként mértük a $^{nat}Ne(\alpha,x)^{22}Na$ folyamat hatáskeresztmetszetét és így 6 új pontot kaptunk a 12.0 MeV ≤ E_α ≤ 22.5 MeV tartományban.

5. Elsőként mértük a $^{nat}Ne(\alpha,x)^{24}Na$ folyamat hatáskeresztmetszetét és ennek során 7 új hatáskeresztmetszetet kaptunk a 2.6 MeV ≤ E_α ≤ 22.5 MeV tartományban.

6. Az $^{40}Ar(\alpha,p)^{43}K$ reakció esetén az első részletesnek tekinthető mérést mi végeztük és annak során 16 energián határoztuk meg a hatáskeresztmetszetet a 8.9 MeV ≤ E_α ≤ 21.4 MeV tartományban. Méréseinkkel együtt így összesen 20 pont áll rendelkezésre a gerjesztési függvényre vonatkozóan.

3. "No-carrier added" ^{24}Na és ^{43}K termelése és a kapcsolódó technikai fejlesztések

1. Az MGC-20E ciklotron egyenes nyalábcsatornájára kiépítettünk egy nagyáramú besugárzások kivitelezésére alkalmas berendezést. A nyalábvéghez kifejlesztettünk egy berillium céltárgyas nagyintenzitású neutronforrást. A berillium céltárgyat 18 MeV energiájú protonokkal bombázva gyorsneutronokat állítottunk elő. A neutronforrással alumínium illetve Al_2O_3 port besugározva ^{24}Na radioizotópot termeltünk az $^{27}Al(n,\alpha)^{24}Na$ reakció révén. Az előállított ^{24}Na -et desztillált vizes mosással nyertük ki majd az oldatot bepároltuk.

2. Az $^{40}Ar(\alpha,p)^{43}K$ reakcióval való ^{43}K termelés céljából megépítettünk a nyalábvéghez egy gázcéltárgyat és hozzá egy gázkört. A céltárgyban keletketkezett ^{43}K nagy részét a kiáramló argon gázzal mostuk ki és a céltárgy közelében elhelyezett enyhén megnedvesített üvegszálas szűrőn fogtuk fel majd arról desztillált vízzel lemostuk. Ezt követően az aktivitást tartalmazó oldatot bepároltuk.

4. Tölgyfák nedváramlásának vizsgálata ^{24}Na és ^{43}K radioizotópos nyomjelzéssel és termometriás módszerrel

Elsősorban a KLTE Ökológia Tanszéke munkatársaival együttműködve kocsánytalan (*Quercus petraea*) és cser (*Quercus cerris*) tölgyek egészséges és beteg fáinak nedváramlását követtük időben radioaktív nyomjelzéses technikával valamint a Granier-féle termometriás módszerrel.

Legfontosabb, közösen elért eredményeinket az alábbiakban adjuk meg.

1. A termelt "no-carrier added" ^{24}Na és ^{43}K radioizotópok desztillált vizes oldatát egészséges és beteg tölgyfák xylem -jében végbemenő vízáramlás nyomjelzésére használtuk terepi körülmények között. Ilyen jellegű vizsgálatokhoz ^{24}Na és ^{43}K izotópokat elsőként mi használtunk. A rövid felezési idők miatt ugyanazokon fákon 10-14 nap múlva megismételhetők a vizsgálatok és a sugárveszély is viszonylag kicsi amennyiben 20 - 50 MBq nagyságrendű aktivitást használunk kísérletenként.

2. Az aktivitás fákba való bejuttatásához egy olyan új injekálási módszert fejlesztettünk ki, mely biztosította, hogy levegőbuborékok ne jussanak be a xylem -be az injektálás során. Ezáltal elkerülhető volt a szállító elemekben a nedváramlás mesterségesen előidézett megszakadása. Az aktivitás eloszlásának változását különböző magasságokban a vizsgált fa törzsére erősített szintillációs detktorokkal követtük.

3. A nedváramlás mérése során a radioaktív nyomjelzéses módszert a Granier-féle termometriás módszerrel kombináltuk. Ilyen összehasonlító vizsgálatokat elsőként mi végeztünk.

4. Gyakran figyeltünk meg a szokásos átlagos napi menetre rakódó, nemegyszer mindössze 5-10 percig detektálható impulzusokat a nedváramlás intenzitásának időfüggésében. Az impulzusok idején az átlagos áramlási sebesség az eredetinek akár többszörösére is megnövekedett majd visszaállt az eredeti szintre.

5. Az impulzusok egészséges *Quercus petraea* valamint beteg *Quercus cerris* fák esetén voltak gyakoribbak míg egészséges *Quercus cerris* és beteg *Quercus petraea* fák esetén ritkábban voltak detektálhatók. Vízzel bőven ellátott fák esetén impulzusok csak igen ritkán figyelhetők meg.

6. A jelenség véleményünk szerint a transpiráció okozta dinamikus vízstresszt tükrözi. A fluktuációk akkor keletkeznek, amikor a fák vízfelvételének és leadásának átmeneti felborulása miatt a tracheákban véletlenszerűen kialakult légemboliák elegendő szabad víz jelenlétében relaxálódni képesek. Ha bőven áll rendelkezésre szabad víz a szövetekben (egészséges *Quercus cerris*), akkor az embolizáció valószínűsége kicsi. Ha kevés a nem kötött víz (beteg *Quercus petraea*), akkor viszont a relaxáció valószínűsége kicsi. A szabad víztartalom bizonyos tartományában az embolizáció és a relaxáció valószínűsége azonos nagyságrendű, ilyenkor gyakoriak a tapasztalt impulzusok. Az egyensúlyi állapothoz tartozó kritikus víztartalom minden bizonnyal fajspecifikus, amint azt az egészséges *Quercus petraea* valamint beteg *Quercus cerris* fák hasonló viselkedése mutatja. A relaxációra néhány órán belül képtelen tracheák nagy száma akár végzetes is lehet a fára nézve, mivel azok végleges eltömődése egy-két napon belül bekövetkezik.

7. Tudomásunk szerint elsőként mutattunk rá arra, hogy nagy gyakorisággal (néhány percenként) folyamatosan mérve az áramlási sebesség fluktuációit a vízstressz kialakulása már a korai szakasztól követhető.

A témához kapcsolódó közlemények

A gerjesztési függvények mérésével kapcsolatos közlemények

1. **Fenyvesi, A.**, Tárkányi, F., Szelecsényi, F., Takács, S., Szűcs, Z., Molnár, T., Sudár, S.
   Measurement of excitation function and thick target yield of the ^{40}Ar(α,p)^{43}K reaction
   Proceedings of the International Conference on Nuclear Data for Science and Technology, Gatlinburg, Tennessee, May 9-13, 1994, Ed.: J. K. Dickens, American Nuclear Society, Inc., 555 N. Kensington Ave., La Grange Park, Illinois 60525, USA, 1994, pp. 406-408.

2. **Fenyvesi, A.**, Tárkányi, F., Szelecsényi, F., Takács, S., Szűcs, Z., Molnár, T., Sudár, S.
   Excitation function and thick target yield of the ^{40}Ar(α,p)^{43}K reaction: production of ^{43}K

Applied Radiation and Isotopes **46**, 1413 (1995).

3. **Fenyvesi, A.**, Merchel, S., Takács, S., Szelecsényi, F., Tárkányi, F. and Qaim, S. M.
Excitation Functions of ^{nat}Ne(^{3}He,x)^{22,24}Na and ^{nat}Ne(α,x)^{22,24}Na Processes: Investigation of Production of ^{22}Na and ^{24}Na at a Medium-Sized Cyclotron
Radiochimica Acta (közlésre elfogadva).

4. **Fenyvesi, A.**, Takács, S., Merchel, S., Pető, G., Szelecsényi, F., Molnár, T., Tárkányi, F. and Qaim, S. M.
Excitation Functions of Charged Particle Induced Reactions on Neon: Relevance to the Production of ^{22,24}Na and ^{18}F
Presented at the *International Conference on Nuclear Data for Science and Technology, 19-24 May, 1997, Trieste, Italy* and submitted for publication in the Proceedings of the Conference (megjelenés alatt).

A fák vízforgalmával kapcsolatos közlemények

5. Béres, Cs., **Fenyvesi, A.**, Jakucs, P., Mahunka, I., Kovács, Z., Molnár, T., Szabó, L., Ditrói, F.
Application of an MGC-20 cyclotron and methods of radioecology in solution of problems of forestry and the wood industry
Nuclear Instruments and Methods in Physics Research **B 43**, 101(1989).

6. **Fenyvesi, A.**, Mahunka, I., Tárkányi, F., Molnár, T., Béres, Cs., Kovács, Z., Mikecz, P., Szűcs, Z.
Production of ^{43}K and ^{24}Na radioisotopes in carrier-free form for use in radioecological studies at the forest area of the Síkfőkút Project
In *Responses of Forest Ecosystems to Environmental Changes*. Eds.: Teller, A., Mathy, P., Jeffers, J.N.R., Elsevier Applied Science, London and New York, 1992, pp. 608-609.

7. Raschi, A., Tognietti, R., Ridder, H.-W., Béres, Cs., **Fenyvesi, A.**
The use of computer thomography in the study of pollution effects on oak trees
Agricoltura Mediterranea, Special Volume, Responses of Plants to Air Pollution, 298(1995).

8. Tognietti, R., Raschi, A., Béres, C., **Fenyvesi, A.**, Ridder, H.-W.
Comparison of sap flow, cavitation and water status of *Quercus petraea* **and** *Quercus cerris* **trees with special reference to computer tomography**
Plant, Cell and Environment **19**, 928 (1996).

9. **Fenyvesi, A.**, Béres Cs., Ridder, H.-W., Raschi A.
Sap-flow velocities and distribution of wet-wood in trunks of healthy and unhealthy *Quercus robur*, *Quercus petraea* **and** *Quercus cerris* **oak trees in Hungary**
Chemosphere (megjelenés alatt).

A 18 MeV p(Be) neutronforrással kapcsolatos közlemények

10. **Fenyvesi, A.**, Mahunka, I., Molnár, T.
Status report on the fast neutron irradiation facility for radiobiological purposes at the Debrecen cyclotron
Zeitschrift für Medizinische Physik **1**, 30 (1991).

11. **Fenyvesi, A.**, Gál, I., Mahunka, I., Molnár, T., Tárkányi, F., Csejtei, A.
Nagyintenzitású ciklotron neutronforrások
Magyar Radiológia **63**, l66 (l989)

12. Molnár, T., **Fenyvesi, A.**, Mahunka, I., Csejtei, A.
Dozimetriai mérések nagyintenzitású ciklotron neutronforrásokon
Magyar Radiológia **63**, l59 (l989)

13. **Fenyvesi, A.**
Az MGC-20 ciklotronra alapozott gyorsneutron források és alkalmazásaik
Egyetemi doktori értekezés
Kossuth Lajos Tudományegyetem, Debrecen, 1990.